



KfG



Application of a conceptual precipitation-runoff model to Himalayan headwatersheds



final Report (DRAFT)

Markus Konz

Kathmandu, December 2003

TABLE OF CONTENTS

TABLE OF CONTENTS.....	1
INTRODUCTION.....	3
CHAPTER I CATCHMENTS CHARACTERISTICS.....	5
I.1 General remarks to Nepal Himalayas.....	5
I.1.1 Physical Features of Nepal.....	5
I.1.2 Climate of Nepal.....	5
I.1.3 River Systems of Nepal.....	5
I.1.4 The Higher Himalaya.....	6
I.1.5 Climatological Characteristics.....	6
I.1.6 Runoff Characteristics.....	7
I.2 Catchments.....	8
I.2.1 Langtang Khola, Langtang.....	10
I.2.2 Modi Khola, Annapurna.....	13
I.2.3 Imja Khola, Khumbu.....	16
I.2.4 Sano Bheri, Kanjiroba.....	18
CHAPTER II DATA BASE.....	19
II.1 Data collection at SGHU.....	19
II.2 Data base of SGHU stations in Langtang, Annapurna, Khumbu and Kanjiroba catchments.....	19
II.3 Rating curves.....	26
II.4 Area Information.....	27
II.5 Reference stations.....	28
CHAPTER III DATA PROCESSING.....	31
III.1 Bridging of data gabs.....	31
III.2 Extrapolation of air-temperature data.....	31
III.2.1 General remarks.....	31
III.2.2 Procedure of extrapolation of daily mean air-temperature values.....	33
III.3 Extrapolation of precipitation data.....	36
III.3.1 General remarks.....	36
III.3.2 Procedure of extrapolation of daily sums of precipitation.....	36

	CHAPTER IV THE HBV3-ETH9 MODEL.....	45
IV.1	Structure of HBV3-ETH9.....	45
IV.2	Parameters of HBV3-ETH9.....	46
IV.3	Snow and glacier routine.....	47
IV.3.1	Differentiation between liquid and solid precipitation.....	47
IV.3.2	Correction of measured precipitation for the compensation of - unsatisfactory representativity of the measurement station - measuring errors for liquid and solid precipitation.....	47
IV.3.3	Estimation of snowmelt.....	48
IV.3.4	Estimation of intensity of orientation dependent ablation of snow cover.....	48
IV.3.5	Estimation of storage and refreezing of liquid water in snow cover.....	50
IV.4	Soil moisture routine and response function.....	50
IV.5	Calibration procedure.....	52
	CHAPTER V RESULTS.....	53
V.1	General remarks.....	53
V.2	Results of the different catchments.....	53
IV.2.1	Langtang Khola, Langtang.....	53
IV.2.2	Modi Khola, Annapurna.....	55
IV.2.3	Imja Khola, Khumbu.....	56
IV.2.4	Sano Bheri, Kanjiroba.....	57
	ACKNOWLEDGEMENTS	59
	LITERATURE.....	61

INTRODUCTION

Nepal is the world's richest country in case of hydropower potentials (Shrestha 1985). With an altitude range of nearly 8800m the hydraulic gradient is enormous. The development of hydropower contributes mainly to the development of the whole country. To improve the assessment of Nepal's hydropower potentials homogenous long time series of precipitation, temperature and discharge are necessary. The Himalayan headwatersheds and their glaciers are the sources of most of Nepal's rivers. Therefore a reliable assessment of water resources in mountainous headwatersheds is important for the assessment of hydropower potentials as well as for drinking water supply. The need for further knowledge of the climatic and hydrologic conditions of mountainous regions as they relate to water and energy resources has been stressed recently by Jauk (2003).

This study is a continuation of the "Snow and Glacier Hydrology Project" initiated by the German Agency for Technical Cooperation in 1987. During this project an earlier version of the conceptual precipitation runoff model HBV-ETH was applied to Langtang Khola, Imja Khola and Modi Khola catchments (Braun et al. 1993, 1998). In the 1998 study an adequate method to bridge gaps in temperature and precipitation time series was developed by Weber (1997). Due to difficult access and harsh conditions of mountainous regions the need of such a procedure is immense. The procedure combines long time data series of the standard meteorological stations at low altitudes with the relatively short data series from high mountain stations to generate continuous data series of daily values of air temperature and precipitation. These data series form the input into a further developed version of the HBV-ETH model. The model algorithm considers detailed area and glacier area distribution in three orientation classes east-west-horizontal, north and south and in altitude belts. This distinction of the topography considers the different contributions to melt water production of each exposition class.

The HBV-ETH model delivers intermediate results concerning catchment precipitation, evaporation, changes in snow and ice storage and changes in soil water storage the main focus is on the spatial and temporal distribution of discharge.

This report is a summary of materials and methods used during the "Nepal Project 2003". It includes a detailed description of the extrapolation algorithms (Weber 1997), the structure of HBV-ETH and of the data base.

CHAPTER I CATCHMENTS CHARACTERISTICS

I.1 General remarks to Nepal Himalayas

I.1.1 Physical Features of Nepal

The kingdom of Nepal is situated in the central part of the Himalayan range. The range separates the Gangetic plains of India from the Tibetan plateau of China. The Himalayan belt extends over 2,400 km from the Punjab Himalayas in the west to the Bhutan and Assam Himalayas in the east. The Nepal Himalayas, situated between 26° 15' to 30° 30' N latitude and 80° 00' to 88° 15' E longitude, stretch from over 800 km northwest to southeast. Their total area of 147,181 km² spans the mountainous region with varying widths of between 90 and 230 km. About 83% of the national land is covered by the rugged terrain of the hills and mountains and the land above 4,500 m is approximately 14.7% of the total land (ICIMOD 2002).

I.1.2 Climate of Nepal

Nepal has a monsoon climate characterized by relatively wet summers and dry winters. Every summer, between June and July, the sun moves northwards and heats up the mountains creating a massive convection cell. The subsequent rising air produces a vacuum that draws the moisture-laden air off the Bay of Bengal. This air runs into the Himalayan barriers, cools as it rises and condenses in the form of rain. Thus begins the monsoon season, which brings three to four months of high humidity with overcast skies and gentle rain. About 70–80% of annual precipitation falls during this period.

The eastern Himalayas receive the brunt of the monsoon, which loses its effect as it moves west along the mountains. Consequently, there is a distinct moisture gradient from east to west.

In winter, western Nepal experiences a reverse monsoon caused by a shift in the jet stream. This phenomenon, which drags weather patterns from the west of the Arabian Sea, brings moisture to the region in the form of snow and is essential for agriculture. The oscillation of the jet stream lasts between November and March and is not only responsible for Everest's snow plume and black appearance but also renders mountaineering difficult (ICIMOD 2002).

I.1.3 River Systems of Nepal

The country receives almost 80% of its annual rainfall within the short period of time of the monsoon season and as such produces a large number of small and big rivers in its mountains. The generation of big and small rivers fed by rainwater, snow melt water, and groundwater leads to the assumption that Nepal is one of the richest countries in the world in terms of hydropower potential. To date, a complete inventory of rivers in Nepal is not available. A study conducted in 1964–65 (Shrestha

1965) indicates that there are over 6,000 rivers in Nepal, of which 960 are more than 10 km long and about 24 of them exceed 100 km in length. The longest river flowing inside Nepal is the Karnali River. Measured along the Mugu branch, the Karnali has a length of 507 km. The average drainage density in Nepal is about 0.3 km/km².

Generally, the rivers in Nepal are classified into three groups on the basis of the source. The first group of rivers is fed by snow and ice melt water as their headwaters are in the snow covered and glaciated region of the High Himalayas. The Koshi, Gandaki, Karnali, and Mahakali rivers fall into this group. These rivers maintain a sustained flow during the dry season and therefore are very important for the development of the nation's water resources. In addition, these rivers contribute a major portion of the flow to the Ganges River during the lean flow period. The second group of rivers originates in the Mahabharat region. They are fed by groundwater during the dry season and therefore do not dry up. The Bagmati, Kamala, Rapti, Mechi, Kankai, and Babai rivers fall into this group. Rivers originating in the Siwalik range fall into the third group, and this includes the Tinau, Banganga, Tilawe, Sirsia, Manusmara, Hardinath, Sunsari and other smaller rivers of the south. The flow in these rivers is significantly low during the dry season, while some of the smaller rivers may dry up completely during the non-monsoon season (ICIMOD 2002).

I.1.4 The Higher Himalaya

The Higher Himalayan zone ranges from 3,000m to more than 8,000m and is mostly covered with snow and glaciers. Out of the 14 peaks in the world higher than 8,000m, The Nepal Himalaya host the eight highest peaks, i.e., Mount Everest, Kanchanjunga, Lhotse, Makalu, Dhaulagiri, Manaslu, Cho-Oyu, and Annapurna I. There are many more higher peaks in the eastern part of Nepal than in the western part. The upper parts of these mountains are formed by Tethys sediments, which are underlain by the central crystalline rocks. The whole range consists mainly of high grade metamorphic rocks like schist and gneiss. Sharp peaks and vertical walled valleys characterize the landforms of this zone (ICIMOD 2002).

I.1.5 Climatological Characteristics

The climate of Nepal is characterized by monsoon circulation, principally easterly winds during the summer, and westerlies from October to May. The summer monsoon, which lasts from June to September, involves a large amount of precipitation. However, the monsoon does not begin abruptly. There is a gradual transition from the dry winter season to the summer monsoon as a result of the pre-monsoon convective rains, which are frequently accompanied by thunderstorms (Kraus 1988). Nepal can be divided into five characteristic climate zones roughly parallel to each other and showing a trend from east to west.

- Hot monsoon climate in the Terai, Inner Terai, and Siwilak regions with a hot and wet summer, and mild and dry winter

- Warm temperate monsoon climate in the Middle Mountains up to a height of about 2,100 m
- Cool temperate monsoon climate in the Middle Mountains and the High Mountains between 2,100 and 3,300 m
- Alpine climate in the High Mountain region up to a height of about 4,800 m
- Tundra type of climate above the snow line where there is perpetual frost and cold desert conditions (Shankar and Shrestha 1985) (ICIMOD 2002).

I.1.6 Runoff Characteristics

The timing of discharge coincides closely with seasonal maxima and minima of precipitation at basin scales. Discharge maxima generally occur in August coinciding with the peak of the monsoon. About 75% of the annual volume of water leaves the respective watershed during the monsoon season (June–September). Minimum values occur during the months of January–May (Alford 1992).

Despite general coincidence in the maxima and the minima in precipitation and stream flow hydrograph, owing to great environmental diversity within the basin, correlation between point-measured precipitation and discharge values is not found. Similarly, the general rule of linear relationship between discharge and basin area is not followed in Nepal.

In addition to intra-annual variations in discharge, rivers in the Himalayan headwaters show diurnal variation. The increase in discharge in the afternoon is due to daytime melting of snow and glacier ice in the catchment. There is an increasing interest in understanding the role played by snow and ice melt in the flow of Himalayan rivers. Particularly, it is important to know the effect of global warming on the regional hydrology. While the country is just beginning to harness the vast hydropower potential estimated at 83 x 106 kW (Shrestha 1985, 1995) changes in the stream flow regimes could negatively impact planning and implementation of hydropower and other water-related structures.

It is expected that the stream flow will increase initially due to rapid melting of snow and glaciers but will drastically decline as the glacier volumes decrease. Nevertheless, any trend in annual volume of water is not yet detected in the rivers of Nepal (Alford 1992). This could be mainly because of large inter-annual variations owing to similar variations in precipitation.

The Himalayan headwaters contain a plethora of glacial lakes, several of them vulnerable to outbursts. The normal flow pattern of these rivers can be significantly altered by a glacial lake outburst flood (GLOF) event. Depending on the nature of the breach and the volume of water released the stream discharge can experience a manifold increase during a GLOF surge (ICIMOD 2002).

I.2 Catchments

The SGHU (Snow and Glacier Hydrology Unit) of DHM (Departement of Hydrology and Meteorology) runs meteorological stations and gauging stations in 6 different catchments. Figure I.1 gives an overview of the location of these catchments.

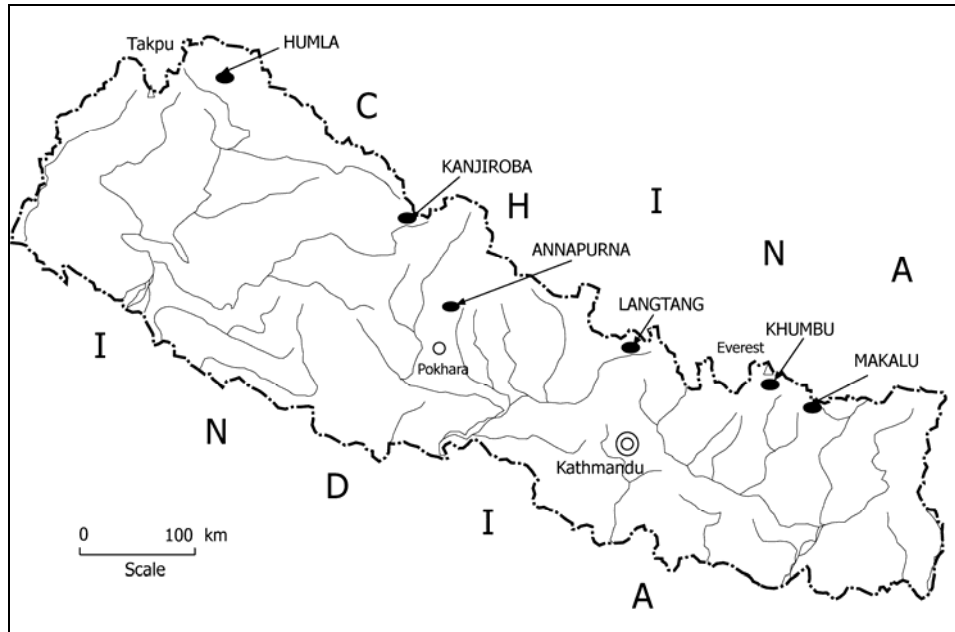


FIG I.1: Map of SGHU stations. Source SGHU.

The investigated catchments in this study are Langtang Khola (Langtang), Imja Khola (Khumbu), Modi Khola (Annapurna) and Sano Bheri (Kanjiroba). Table I.1 gives a description of the catchments with the location of meteorological station and hydrological station and the catchment area and glacier area of each catchment name, longitude, latitude and altitude of the stations are taken from SGHU Yearbook 1999-2000 area and glacier area information are derived from digital models of the catchments, for more information about the digital elevation models please refer to chapter II. In table I.2 the main glaciers of each catchment are marked with a number which are also added to the maps of the catchments below. The glacier information are taken from ICIMOD 2002

Tab. I.1: Description of the catchments.

Name of station and catchment	Location						Catchment area (km ²)	Glacier covered area (km ²)
	Meteorological station			Hydrological station				
	Lat. (N)	Long. (E)	Alt. (m)	Lat. (N)	Long. (E)	Alt. (m)		
Langtang Khola Langtang								
Kyangjing	28 13 00	85 37 00	3920	28 13 00	85 33 00	3800	360	165
Modi Khola Annapurna								
MBC *	28 32 00	83 57 00	3470				160	76
Bagar				28 31 00	83 57 00	3160		
Imja Khola Khumbu								
Dingboche	27 53 20	86 56 40	4355	27 53 40	86 56 40	4375	141	53
Sano Bheri Kanjiroba								
Hurikot	29 07 00	82 36 00	2735					
Kaigaon				29 05 00	82 33 00	2600		

* MBC Machhapuchhare Base Camp

Tab. I.2: Glaciers of the catchments.

Name of station and catchment	Glaciers of catchment Map No.	Area (km ²)	Mean length (m)	Mean elevation (m)	Orientation of ablation	Orientation of accumulation
Langtang Khola Langtang	1	12	6580	5522	S	SE
	2	6	5830	5136	SW	SW
	3	5	1520	5841	SW	SW
	4	16	11590	4991	SE	SE
	5	68	17740	5833	S	S
	6	4	2150	5737	SW	SW
	7	26	1580	5243	SW	SW
Modi Khola Annapurna	1	5	2530	5685	NE	NE
	2	8	5060	5105	SE	SE
	3	3	2720	5441	SE	SE
	4	10	12670	5876	S	S
	5	1	1200	5547	W	W
	6	1	1450	5151	SW	SW
	7	2	3140	5486	SE	SE
	8	12	8260	5429	S	S
	9	4	3800	5898	S	S
	10	15	6970	5830	SW	SW
	11	3	3160	5395	NW	NW
	12	1	1900	5319	W	W
	13	3	3215	5471	W	W
Imja Khola Khumbu	1	5	6330	5349	S	S
	2	2	4110	5349	S	S
	3	9	8870	5465	SW	SW
	4	19	10770	6431	W	SW
	5	4	4110	5508	NW	NW
	6	6	5060	5525	N	N
Sano Bheri Kanjiroba	Not calculated					

I.2.1 Langtang Khola, Langtang

The Langtang Khola catchment is located close to Kathmandu and contains 3 peaks over 7000m and many more 6000m high peaks. Together with Khumbu and Annapurna the Langtang valley is one of Nepal's most popular trekking areas. In 1971 Langtang became Nepal's first National Park.

The map in figure I.2 shows the boundary of the Langtang Khola catchment with all important glaciers. A detailed description of the glaciers with numbers is given in table I.2 on page 5.

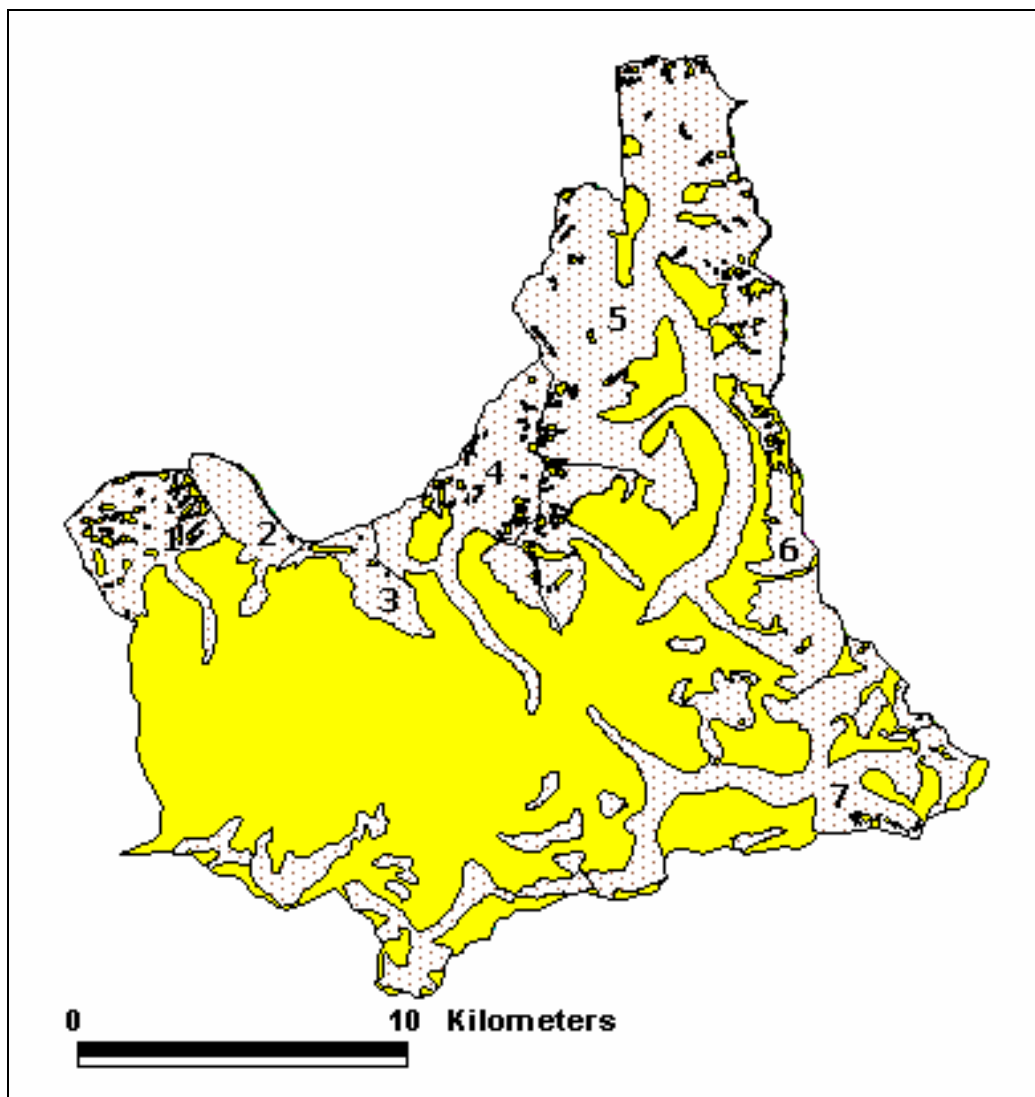


Fig. I.2: Map of Langtang Khola catchment with the glaciers. Glaciers with numbers are described in table I.2 on page 5.

The HBV3-ETH9 model requires several area information, as described in chapter 4. The following tables and diagrams give information about area distribution in North, South and East-West- Horizontal exposition and in 500m altitude belts.

Tab. I.3: Area distribution of Langtang Khola catchment derived from digital maps of Survey Department and from DAV Alpenvereinskarte Langthang Himal, Ost.

Exposition class	Altitude belt [m]	Area [km ²]
N	3500-4000	5.2
N	4000-4500	11.6
N	4500-5000	19.9
N	5000-5500	27.0
N	5500-6000	11.5
N	6000-6500	4.6
N	6500-7000	0.5
N	7000-7500	0.0
S	3500-4000	4.5
S	4000-4500	11.6
S	4500-5000	22.8
S	5000-5500	32.1
S	5500-6000	22.3
S	6000-6500	8.8
S	6500-7000	1.3
S	7000-7500	0.0
EWH	3500-4000	3.8
EWH	4000-4500	16.0
EWH	4500-5000	45.1
EWH	5000-5500	57.1
EWH	5500-6000	38.2
EWH	6000-6500	13.0
EWH	6500-7000	2.9
EWH	7000-7500	0.1

Tab. I.4: Glacier distribution of Langtang Khola catchment derived from digital maps of Survey Department and from DAV Alpenvereinskarte Langthang Himal, Ost.

Exposition class	Altitude belt [m]	Area [km ²]
N	4000-4500	0.3
N	4500-5000	5.0
N	5000-5500	13.2
N	5500-6000	6.0
N	6000-6500	2.8
N	6500-7000	0.4
N	7000-7500	0.0
S	3500-4000	0.0
S	4000-4500	1.7
S	4500-5000	7.1
S	5000-5500	16.6
S	5500-6000	16.6
S	6000-6500	6.3
S	6500-7000	1.0
S	7000-7500	0.0
EWH	3500-4000	0.1
EWH	4000-4500	2.0
EWH	4500-5000	14.8
EWH	5000-5500	30.5
EWH	5500-6000	29.2
EWH	6000-6500	9.2
EWH	6500-7000	2.4
EWH	7000-7500	0.1

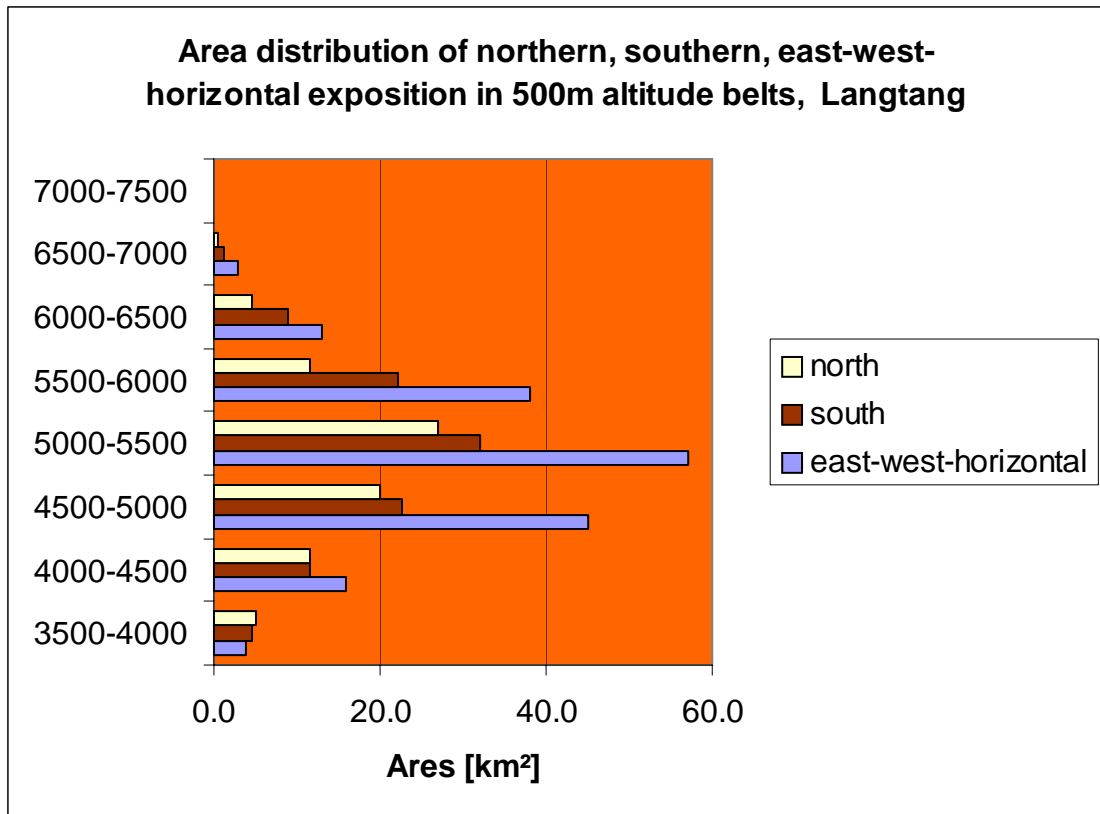


Fig. I.3: Bar diagram to visualize the area distribution Langtang Khola catchment, Langtang derived from digital maps of Survey Department and from DAV Alpenvereinskarte Langthang Himal, Ost.

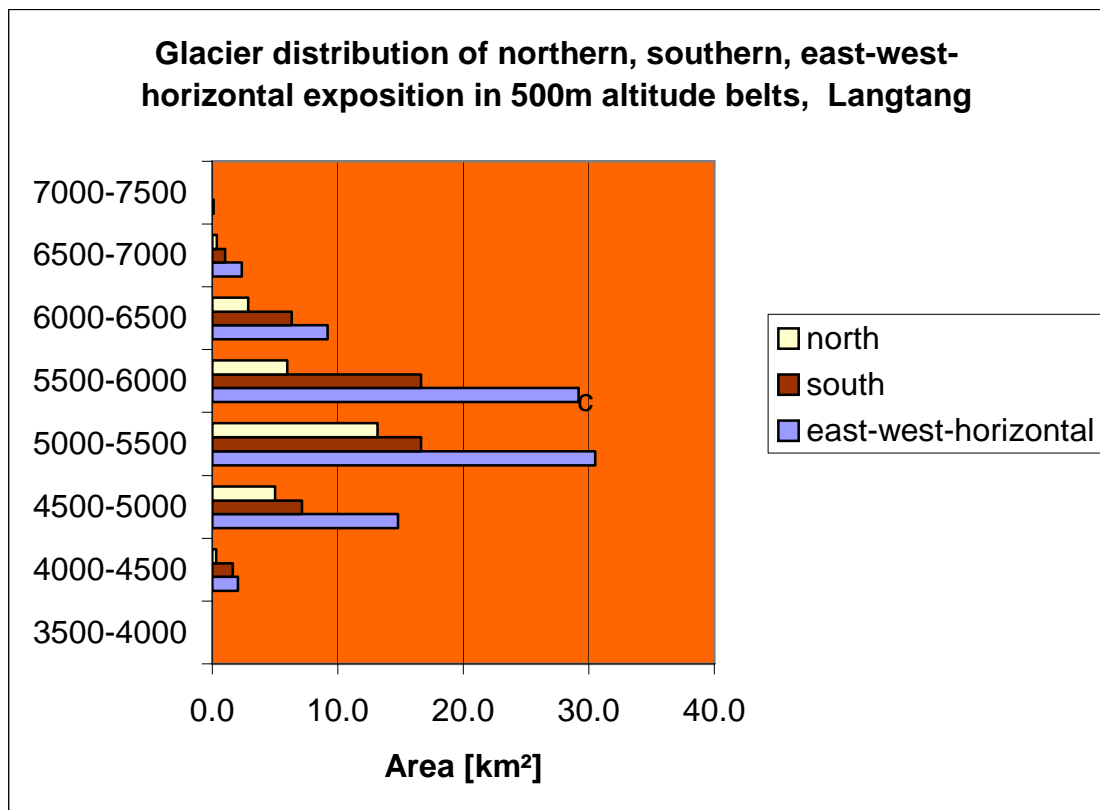


Fig. I.4: Bar diagram to visualize the Glacier distribution of Langtang Khola catchment, Langtang derived from digital maps of Survey Department and from DAV Alpenvereinskarte Langthang Himal, Ost.

I.2.2 Modi Khola, Annapurna

There is one of the highest peak of the world located in the Annapurna catchment, the Annapurna I. 6 peaks are higher than 7000m. Annapurna Base Camp and Machhapuchhare Base Camp are popular trekking destinations and are located within the catchment.

Figure I.5 shows a map with the catchment boundaries and the main glaciers are marked with numbers which are explained in table I.2 an page 5.

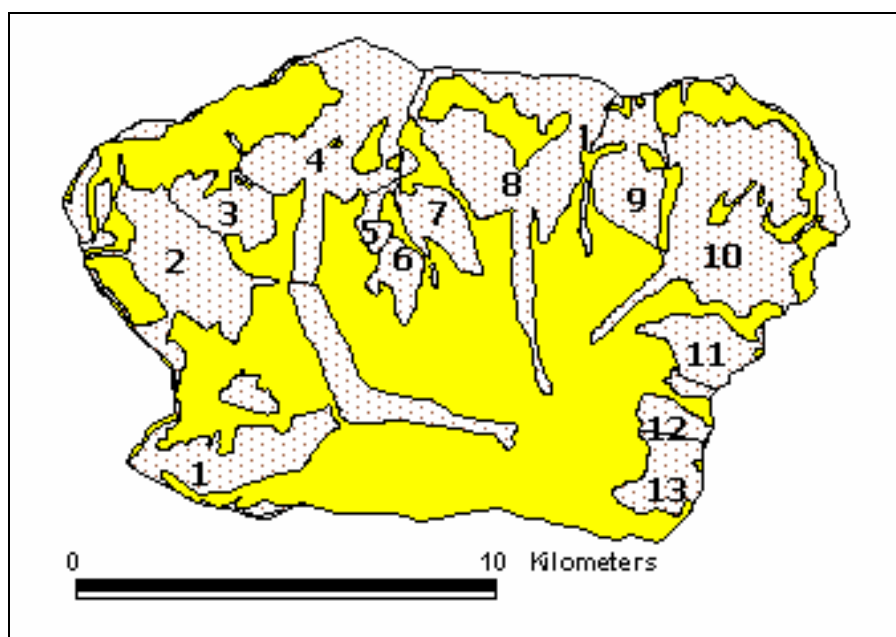


Fig. I.5: Map of Modi Khola catchment with glaciers. Glaciers with numbers are described in table I.2 an page 5.

The area distribution is summarized in tables I.5 and I.6 and visualised in figure I.6 and I.7.

Tab. I.5: Area distribution of Modi Khola catchment derived from digital maps of Survey Department.

Exposition class	Altitude belt [m]	Area [km ²]
N	3000-3500	0.0
N	3500-4000	1.1
N	4000-4500	5.4
N	4500-5000	6.6
N	5000-5500	4.4
N	5500-6000	3.4
N	6000-6500	1.0
N	6500-7000	0.4
N	7000-7500	0.1
N	7500-8000	0.0
S	3000-3500	0.1
S	3500-4000	1.4
S	4000-4500	6.5
S	4500-5000	9.3
S	5000-5500	13.1
S	5500-6000	9.9

S	6000-6500	7.8
S	6500-7000	6.9
S	7000-7500	3.0
S	7500-8000	1.0
EWH	3000-3500	0.2
EWH	3500-4000	2.9
EWH	4000-4500	10.8
EWH	4500-5000	17.1
EWH	5000-5500	19.9
EWH	5500-6000	14.4
EWH	6000-6500	7.9
EWH	6500-7000	3.9
EWH	7000-7500	1.9
EWH	7500-8000	0.2

Tab. I.6: Glacier distribution of Modi Khola catchment derived from digital maps of Survey Department.

Exposition class	Altitude belt [m]	Area [km ²]
N	3500-4000	0.4
N	4000-4500	0.6
N	4500-5000	1.5
N	5000-5500	1.7
N	5500-6000	1.4
N	6000-6500	0.7
N	6500-7000	0.2
N	7000-7500	0.1
N	7500-8000	0.0
S	3500-4000	0.4
S	4000-4500	2.4
S	4500-5000	2.9
S	5000-5500	10.3
S	5500-6000	7.0
S	6000-6500	3.7
S	6500-7000	3.7
S	7000-7500	1.4
S	7500-8000	0.5
EWH	3500-4000	0.6
EWH	4000-4500	2.6
EWH	4500-5000	4.6
EWH	5000-5500	13.2
EWH	5500-6000	9.5
EWH	6000-6500	3.9
EWH	6500-7000	2.1
EWH	7000-7500	1.0
EWH	7500-8000	0.1

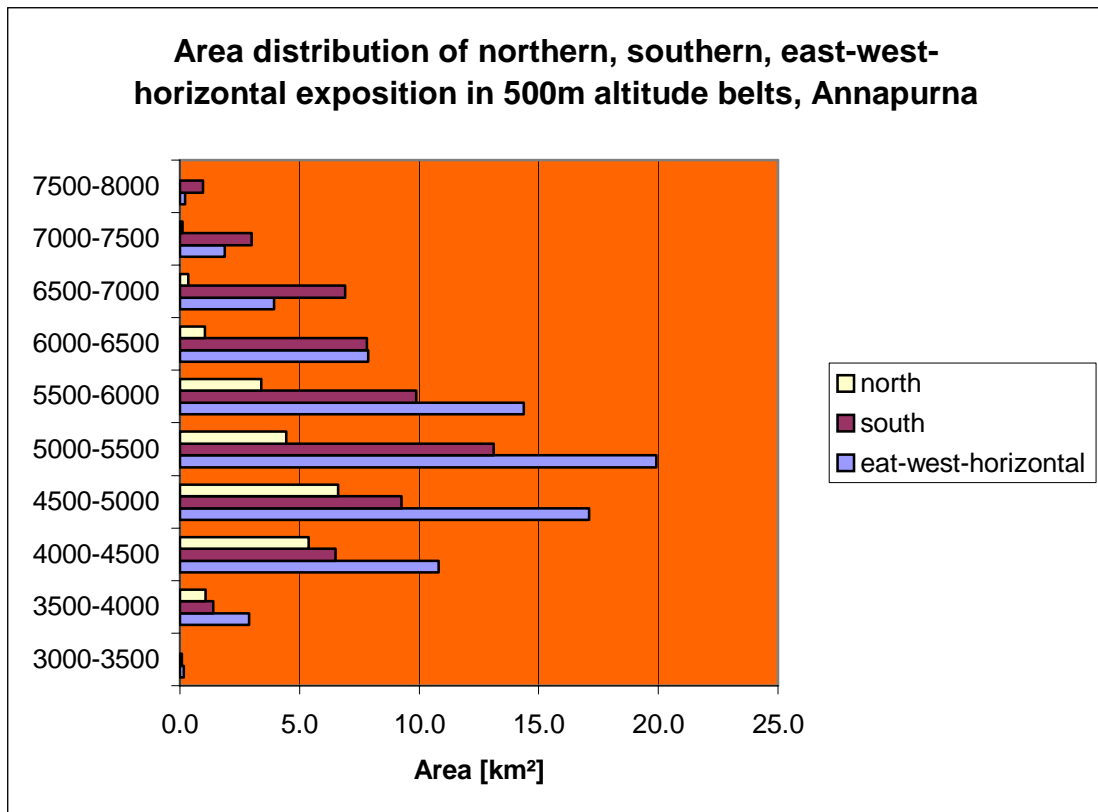


Fig. I.6: Bar diagram to visualize the area distribution of Modi Khola catchment, Annapurna derived from digital maps of Survey Department.

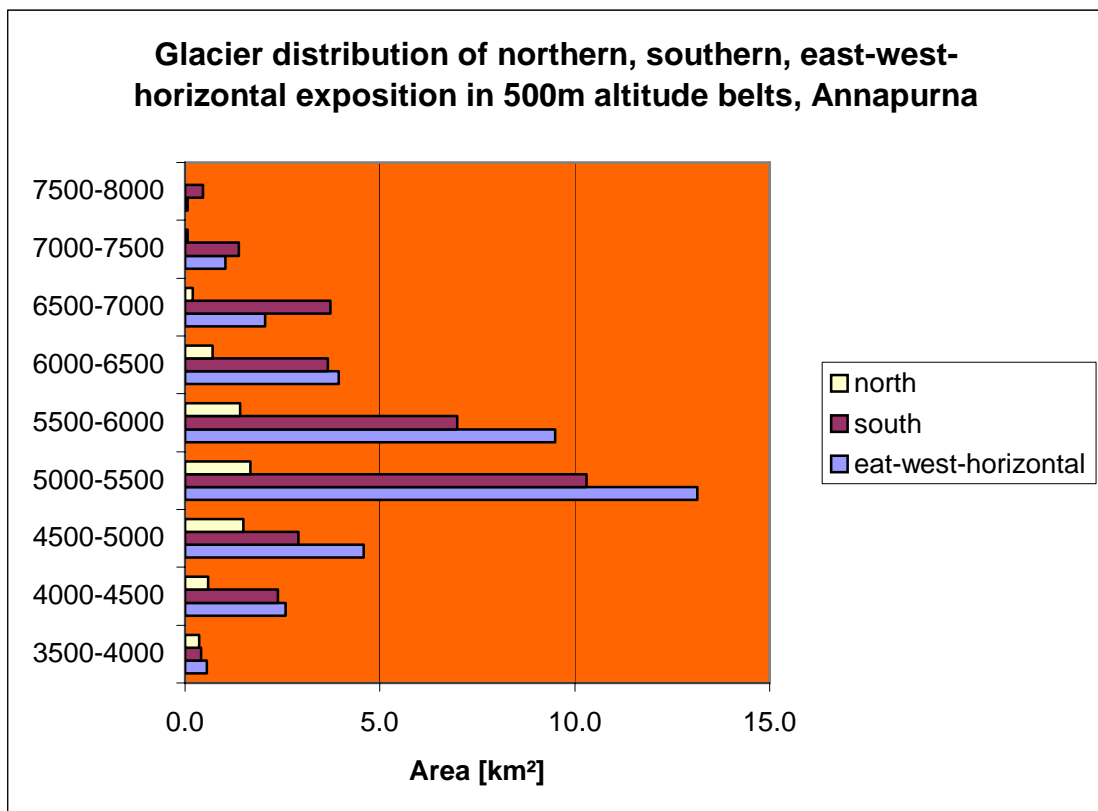


Fig. I.7: Bar diagram to visualize the glacier distribution of Modi Khola catchment, Annapurna derived from digital maps of Survey Department.

I.2.3 Imja Khola, Khumbu

Two of world's 14 eight-thousand meter peaks – Lhotse and Lhotse Shar - are located in the Imja Khola catchment. The surrounding is dominated by the empty-standing Ama Dablam a 6800m high pyramid. The Solo-Khumbu region is Nepal's most famous trekking and mountaineering region home of the Everest and the Sherpa people.

The map in figure I.8 shows the boundary of the Imja Khola catchment with all important glaciers. A detailed description of the glaciers with numbers is given in table I.2 on page 5.

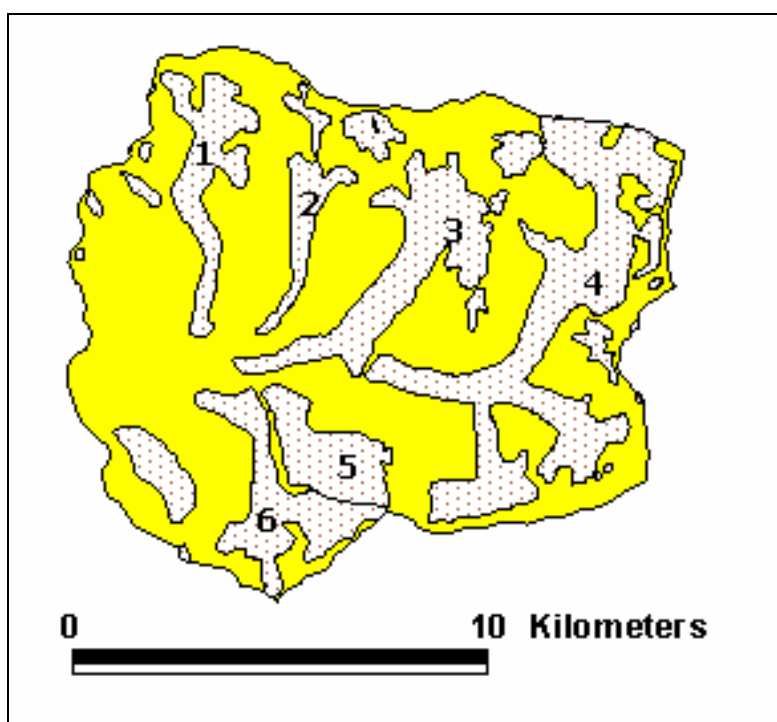


Fig. I.8: Map of Imja Khola catchment with the glaciers. Glaciers with numbers are described in table I.2 on page 5.

Tables I.7 and I.8 show a summary of the area distribution of the catchment and the information is visualized in figures I.9 and I.10.

Tab. I.7: Area distribution of Imja Khola catchment derived from digital maps of Survey Department.

Exposition class	Altitude belt [m]	Area [km ²]
N	4000-4500	0.3
N	4500-5000	5.6
N	5000-5500	13.4
N	5500-6000	5.7
N	6000-6500	1.6
N	6500-7000	0.5
N	7000-7500	0.0
N	7500-8000	0.0
N	8000-8500	0.0
S	4000-4500	0.6

S	4500-5000	6.0
S	5000-5500	20.2
S	5500-6000	8.3
S	6000-6500	4.4
S	6500-7000	3.9
S	7000-7500	3.4
S	7500-8000	1.4
S	8000-8500	0.3
S	8500-	0.0
EWB	4000-4500	0.3
EWB	4500-5000	8.4
EWB	5000-5500	36.3
EWB	5500-6000	13.6
EWB	6000-6500	4.3
EWB	6500-7000	1.9
EWB	7000-7500	0.7
EWB	7500-8000	0.3
EWB	8000-8500	0.1

Tab. I.8: Glacier distribution of Imja Khola catchment derived from digital maps of Survey Department.

Exposition class	Altitude belt [m]	Area [km ²]
N	4500-5000	2.3
N	5000-5500	6.7
N	5500-6000	1.6
N	6000-6500	0.1
N	6500-7000	0.0
N	7000-7500	0.0
N	7500-8000	0.0
S	4500-5000	1.1
S	5000-5500	9.6
S	5500-6000	2.2
S	6000-6500	1.0
S	6500-7000	2.3
S	7000-7500	1.5
S	7500-8000	0.4
EWB	4500-5000	3.2
EWB	5000-5500	15.3
EWB	5500-6000	4.0
EWB	6000-6500	0.9
EWB	6500-7000	0.9
EWB	7000-7500	0.3
EWB	7500-8000	0.0

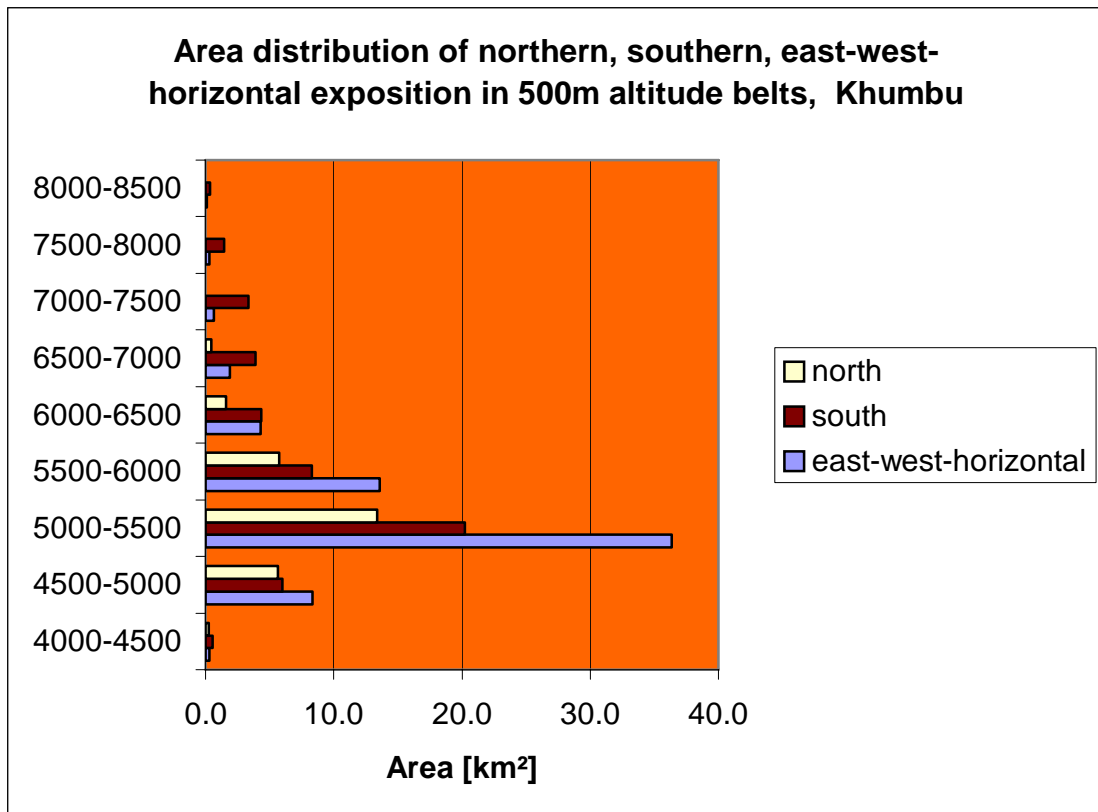


Fig. I.9: Bar diagram to visualize the area distribution of Imja Khola catchment, Khumbu derived from digital maps of Survey Department.

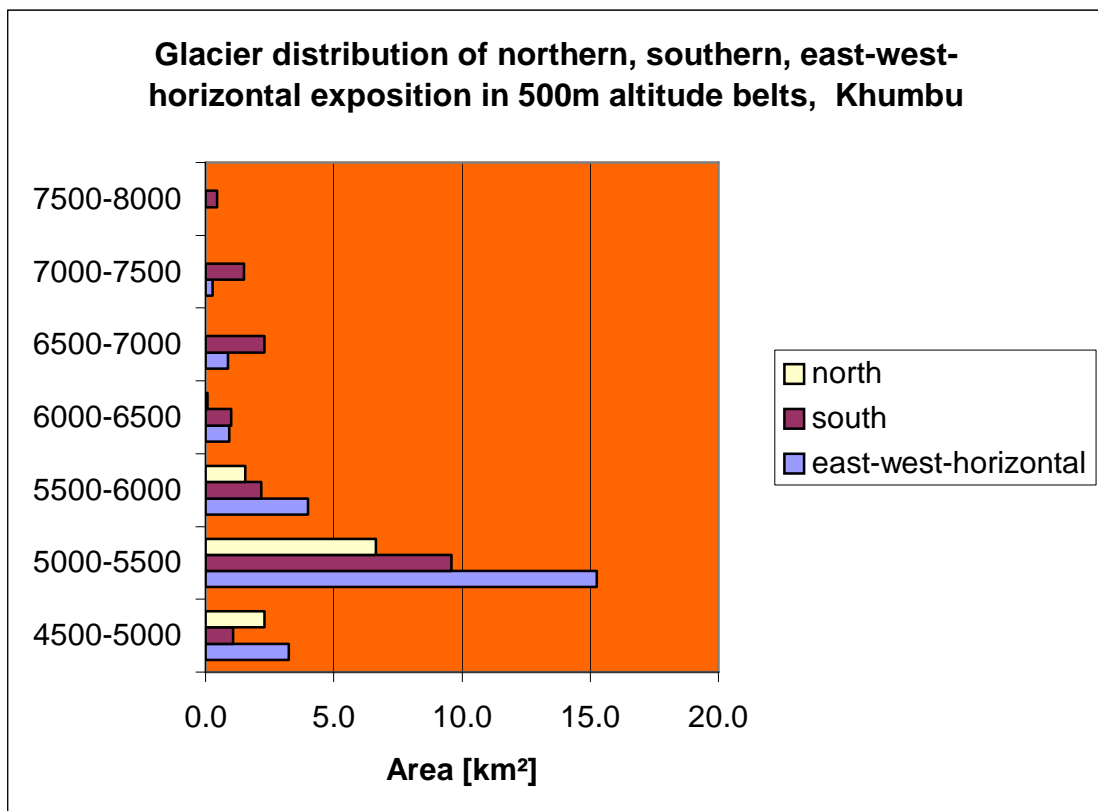


Fig. I.10: Bar diagram to visualize the glacier distribution of Imja Khola catchment, Khumbu derived from digital maps of Survey Department.

I.2.4 Sano Bheri, Kanjiroba not calculated so far

CHAPTER II DATA BASE

II.1 Data collection at SGHU

Snow and Glacier Hydrology investigation has started in 1987 by the Department of Hydrology and Meteorology (DHM) in collaboration with GTZ within the framework of study and expert fund provided by the government of Germany (Grabs and Pokhrel 1993). During this period three hydrometeorological stations were established in Annapurna, Langtang and Khumbu regions with the purpose of systematic collection of hydrological and meteorological data. Up to now further stations were established and the project is undertaken by His Majesty's Government of Nepal and running through the resources of its own.

Discharge is measured by 4-hourly gauge height and by dilution techniques to derive rating curves and deduce stage-flow-relation published as daily mean values. Temperature is measured 6-hourly and published as maximum, minimum and mean daily temperature. Precipitation is recorded as daily total.

The SGHU stations also record radiation, wind speed and humidity. These data are not needed to calculate runoff with HBV3-ETH9.

Data are published in yearbooks by His Majesty's Government of Nepal, Ministry of Science and Technology, Department of Hydrology and Meteorology, Snow and Glacier Hydrology Section, Kathmandu, Nepal.

II.2 Data base of SGHU stations in Langtang, Annapurna, Khumbu and Kanjiroba catchments

Most of the stations of the Snow and Glacier Hydrology Unit, are situated in higher Himalayan region. The access to these higher Himalayan catchments is complicated and it takes a long travel to reach the gauging stations from Kathmandu. Due to that fact the data collection of SGHU stations has been outsourced to local staff living close to the station. These data collectors are originally farmers or mountain guides and are not familiar to the scientific demand for reliable data basis. The environmental condition in high alpine Himalayas is rough, too. There are a lot of data gaps caused by avalanches, hail, thunderstorms or heavy rainfall during monsoon season. These heavy weather events causes considerable damage to the station and the instruments. Vandalism by local people and animals is also a reason for data losses.

SGHU has made a lot of efforts to improve data collection and to keep the stations operational throughout the whole year. Emergency field visits in addition to regular field visits and local staff training are some of these efforts to provide more reliable data. Despite of this, remoteness and inaccessibility of stations during monsoon and winter season mainly due to floods, avalanches and heavy snowfall sometimes delay the maintenance work of the stations.

The availability of hydro-meteorological data varies from catchment to catchment. The number of days of missing data of the treated catchments are summarized in tables II.1, II.2, II.3, II.4. As complete meteorological data files are a prerequisite

for successful application of the HBV3-ETH9 precipitation-runoff model, missing values were interpolated by using additional data from stations in the vicinity of the catchment (chapter III).

Tab. II.1: Number of days of missing data, Langtang Khola catchment, Langtang.

Hydrological year	Air temperature	Precipitation	Stage (waterlevel)
1987/88	Okt.: 14 days	Nov.: 30 days	Mar.: 8 days
	Nov.: 30 days		May.: 1 day
	Dec.: 7 days		Jun.: 1 day
	Jan.: 2 days		Jul.: 1 day
	Mar.: 2 days		Aug.: 1 day
	Jun.: 2 days		Sep.: 1 day
	Jul.: 2 days		Oct.: 2 days
	Aug.: 1 day		Nov.: 1 day
			Dec.: 2 days
Sum	60 days	30 days	18 days
1988/89	Jan.: 1 day	0 days	Jan.: 13 days
	Mar.: 1 day		Feb.: 8 days
	Aug.: 2 days		Mar.: 1 day
			Apr.: 1 day
			Jun.: 1 day
			Jul.: 6 days
			Aug.: 7 days
			Sep.: 5 days
			Oct.: 7 days
		Nov.: 1 day	
		Dec.: 2 days	
Sum	4 days	0 days	52 days
1989/90	0 days	Dec.: 31 days	Jan.: 17 days
		Jul.: 30 days	Jul.: 7 days
Sum	0 days	61 days	24 days
1990/91	Jan.: 1 day	Jan.: 31 days	Apr.: 5 days
		Feb.: 28 days	May.: 11 days
		Mar.: 30 days	Jun.: 6 days
		Jun.: 3 days	Jul.: 5 days
		Aug.: 3 days	Aug.: 3 days
		Sep.: 27 days	Sep.: 26 days
			Nov.: 1 day
			Dec.: 2 days
	Sum	1 day	122 days
1991/92	Sep.: 3 days	Oct.: 2 days	Jan.: 10 days
		Nov.: 1 day	Feb.: 6 days
		Jul.: 2 days	Oct.: 3 days
		Aug.: 1 day	Nov.: 4 days
			Dec.: 7 days
Sum	3 days	6 days	30 days
1992/93	May : 1 day	Sep.: 1 day	Jan.: 3 days
			Feb.: 1 day
			Mar.: 2 days
			Apr.: 2 days
			May.: 4 days
			Jun.: 6 days
			Jul.: 3 days
			Sep.: 7 days
	Sum	1 day	1 day
1993/94	0 days	Feb.: 1 day	Feb.: 3 days
		Jul.: 28 days	Apr.: 2 days
		Aug.: 1 day	Jun.: 1 day
			Jul.: 3 days
		Oct.: 7 days	
Sum	0 days	30 days	16 days
1994/95	0 days	Oct.: 31 days	Feb.: 1 day
		Nov.: 30 days	Mar.: 1 day
		Dec.: 31 days	Apr.: 1 day
Sum	0 days	92 days	3 days
1995/96	Feb.: 1 day	0 days	Feb.: 2 days
			Apr.: 1 day
			Jun.: 6 days

			Jul.: 3 days
			Aug.: 6 days
			Sep.: 2 days
Sum	1 day	0 days	20 days
1996/97	Sep.: 3 days	0 days	Jan.: 2 days
			Feb.: 6 days
			Apr.: 4 days
			May.: 1 day
			Jun.: 6 days
			Sep.: 1 days
			Oct.: 4 days
			Nov.: 1 day
Sum	3 days	0 days	25 days
1997/98	Jan.: 1 day	Feb.: 1 day	Jan.: 2 days
	Aug.: 3 days		Feb.: 1 day
			Mar.: 8 days
			Apr.: 2 days
			May.: 13 days
			Jun.: 8 days
			Jul.: 2 days
			Aug.: 7 days
			Sep.: 4 days
			Oct.: 3 days
			Nov.: 2 days
			Dec.: 21 days
Sum	4 days	1 day	73 days
1998/99	Dec.: 3 days	0 days	Jan.: 31 days
	May : 4 days		Feb.: 28 days
	Jul.: 2 days		Mar.: 31 days
			Apr.: 30 days
			May.: 31 days
			Jun.: 30 days
			Jul.: 31 days
			Aug.: 31 days
			Sep.: 30 days
			Oct.: 7 days
			Dec.: 1 day
Sum	9 days	0 days	281 days
1999/00	Oct.: 2 days	Feb.: 1 day	Jan.: 31 days
	Feb.: 1 day	Jul.: 5 days	Feb.: 28 days
	Jul.: 2 days		Mar.: 31 days
	Aug.: 1 day		Apr.: 30 days
			May.: 31 days
			Jun.: 30 days
			Jul.: 31 days
			Aug.: 31 days
			Sep.: 30 days
			Oct.: 31 days
			Nov.: 30 days
			Dec.: 31 days
Sum	6 days	6 days	365 days

Tab. II.2: Number of days of missing data, Modi Khola catchment, Annapurna.

Hydrological year	Air temperature	Precipitation	Stage (waterlevel)
1991/92	Nov.: 2 days	Okt.: 24 days	Dec.: 12 days
		Nov.: 30 days	Jan.: 31 days
		Dec.: 31 days	Feb.: 29 days
		Mar.: 21 days	Mar.: 31 days
		Apr.: 19 days	Apr.: 30 days
		May.: 27 days	May.: 31 days
		Jun.: 16 days	Jun.: 7 days
			Jul.: 14 days
			Aug.: 19 days
			Sep.: 3 days
Sum	2 days	168 days	207 days
1992/93	Jan.: 1 day	Mar.: 17 days	Oct.: 17 days
	Aug.: 2 days	Apr.: 11 days	Nov.: 9 days
		Jun.: 9 days	Dec.: 16 days
		Jul.: 16 days	Jan.: 31 days
		Aug.: 4 days	Feb.: 18 days
		Sep.: 4 days	Mar.: 19 days

			Apr.: 30 days
			May.: 31 days
			Jun.: 30 days
			Jul.: 19 days
			Sep.: 3 days
Sum	3 days	61 days	223 days
1993/94	Dec.: 2 days	Oct.: 1 day	Oct.: 31 days
	Jan.: 2 days	Nov.: 10 days	Nov.: 26 days
		Dec.: 31 days	Dec.: 6 days
		May.: 8 days	Jan.: 1 day
		Jun.: 5 days	Feb.: 27 days
		Jul.: 9 days	Mar.: 31 days
			Apr.: 29 days
			May.: 27 days
			Jun.: 27 days
			Jul.: 26 days
			Aug.: 24 days
			Sep.: 23 days
Sum	4 days	64 days	278 days

Tab. II.3: Number of days of missing data, Imja Khola catchment, Khumbu.

Hydrological year	Air temperature	Precipitation	Stage (waterlevel)
1987/88	Nov.: 19 days	Nov.: 30 days	Oct.: 13 days
	Jan.: 24 days	Jan.: 31 days	Jan.: 30 days
	Feb.: 15 days		Aug.: 21 days
	May.: 16 days		Sep.: 30 days
	Jun.: 1 day		
	Jul.: 3 days		
	Aug.: 10 days		
	Sep.: 1 day		
Sum	89 days	61 days	94 days
1988/89	Okt.: 1 day	Dec.: 31 days	Oct.: 4 days
	Feb.: 7 days	Jan.: 31 days	Jun.: 6 days
	Mar.: 12 days		
	Apr.: 5 days		
Sum	25 days	62 days	10 days
1989/90	Dec.: 3 days	Dec.: 31 days	Mar.: 1 day
	Mar.: 2 days		
	Apr.: 23 days		
	May.: 31 days		
	Jun.: 30 days		
	Jul.: 12 days		
Sum	101 days	31 days	1 day
1990/91	Okt.: 1 day	Aug.: 4 days	0 days
	Jan.: 12 days	Sep.: 30 days	
	Mar.: 2 days		
	May.: 10 days		
	Sep.: 3 days		
Sum	28 days	34 days	0 days
1991/92	Okt.: 8 days	Okt.: 16 days	Oct.: 12 days
	Nov.: 4 days	Nov.: 12 days	Nov.: 30 days
	Dec.: 2 days		Dec.: 31 days
	Jan.: 5 days		
	Feb.: 9 days		
	Mar.: 3 days		
	Apr.: 10 days		
	May.: 2 days		
	Jun.: 5 days		
	Jul.: 5 days		
	Aug.: 2 days		
	Sep.: 3 days		
Sum	58 days	28 days	73 days
1992/93	Okt.: 7 days	Jan.: 9 days	Jan.: 2 days
	Dec.: 10 days	Feb.: 18 days	Feb.: 28 days
	Aug.: 1 day	Mar.: 24 days	Mar.: 2 days
			Sep.: 30 days
Sum	18 days	51 days	62 days
1993/94	Dec.: 1 day	0 days	Oct.: 31 days
	May.: 1 day		Nov.: 30 days
	Jun.: 2 days		Dec.: 31 days
			Jan.: 24 days

Sum	4 days	0 days	116 days
1994/95	Jun.: 1 day	0 days	0 days
Sum	1 day	0 days	0 days
1995/96	Okt.: 12 days Dec.: 4 days Feb.: 1 day Apr.: 1 day Jun.: 1 day Aug.: 1 day	Jan.: 31 days Feb.: 29 days Mar.: 31 days Apr.: 30 days May.: 31 days Jun.: 30 days Jul.: 31 days Aug.: 31 days Sep.: 30 days	Jan.: 31 days Feb.: 28 days Mar.: 31 days Apr.: 30 days May.: 31 days Jun.: 31 days
Sum	20 days	274 days	182 days
1996/97	Okt.: 5 days Nov.: 10 days Dec.: 1 day	Okt.: 31 days Nov.: 30 days Dec.: 31 days Jan.: 31 days Feb.: 28 days Mar.: 31 days Apr.: 30 days May.: 31 days Jun.: 30 days Aug.: 1 day Sep.: 3 days	Oct.: 1 day Nov.: 1 day Jan.: 1 day Mar.: 31 days Apr.: 30 days May.: 31 days Jul.: 1 day Aug.: 1 day
Sum	16 days	277 days	97 days
1997/98	Apr.: 3 days	Okt.: 31 days Aug.: 31 days Sep.: 30 days	Oct.: 1 day Dec.: 31 days Jun.: 8 days Jul.: 31 days Aug.: 31 days Sep.: 30 days
Sum	3 days	92 days	132 days
1998/99	Nov.: 7 days Dec.: 31 days May.: 1 day Jun.: 13 days Aug.: 1 day	Okt.: 31 days Nov.: 30 days Dec.: 31 days Jan.: 31 days Feb.: 28 days Mar.: 31 days Apr.: 30 days May.: 31 days Jun.: 30 days Jul.: 31 days Aug.: 31 days Sep.: 30 days	Oct.: 31 days Nov.: 30 days Dec.: 31 days
Sum	53 days	365 days	92 days

Tab. II.4: Number of days of missing data, Sano Bheri catchment, Kanjiroba.

hydrological year	air temperature	precipitation	stage (waterlevel)
1991/92	0 days	Dec.: 8 days Jan.: 5 days	Dec.: 9 days Jan.: 31 days Feb.: 29 days Mar.: 31 days Apr.: 30 days Mai.: 31 days Jun.: 30 days Jul.: 31 days Aug.: 31 days Sep.: 30 days
Sum	0 days	13 days	283 days
1992/93	0 days	Jan.: 24 days Jun.: 4 days Jul.: 4 days	Oct.: 31 days Nov.: 30 days Dec.: 31 days Jan.: 31 days Feb.: 28 day Mar.: 31 days Apr.: 30 days Mai.: 7 days Jun.: 15 days Jul.: 6 days Sep.: 3 days
Sum	0 day	32 day	243 days

1993/94	0 days	Dec.: 23 days Feb.: 12 days Jul.: 24 days Aug.: 26 days Sep.: 15 days	Oct.: 7 days Nov.: 8 days Dec.: 31 days Jan.: 31 days Feb.: 29 days Mar.: 31 days Apr.: 30 days Mai.: 31 days Jun.: 30 days Jul.: 31 days Aug.: 31 days Sep.: 30 days
Sum	0 days	100 days	320 days
Gauging station shifted from Kaigoan to Hurrikot December 1994			
1994/95	Feb.: 1 day Mar.: 19 days	Jan.: 31 days Feb.: 28 days Mar.: 31 days Apr.: 30 days Mai.: 31 days Jun.: 30 days Jul.: 31 days Aug.: 31 days Sep.: 30 days	Oct.: 31 days Nov.: 30 days Dec.: 31 days Jan.: 31 days Feb.: 28 days
Sum	20 days	273 days	151 days
1995/96	Nov.: 7 days Dec.: 2 days Feb.: 6 days Mar.: 19 days Apr.: 1 day	Oct.: 31 days Nov.: 30 days Dec.: 31 days Jan.: 31 days Feb.: 29 days Mar.: 31 days Apr.: 30 days Mai.: 31 days Jun.: 30 days Jul.: 31 days Aug.: 31 days Sep.: 30 days	Jan.: 2 days
Sum	35 day	366 days	2 days
1996/97	Nov.: 7 days Dec.: 22 days	Oct.: 31 days Nov.: 30 days Dec.: 31 days Jul.: 18 days Sep.: 11 days	Aug.: 4 days
Sum	29 days	121 days	4 days
1997/98	Oct.: 10 days Nov.: 9 days Dec.: 5 days	Dec.: 10 days Jan.: 31 days Mai.: 1 day	Jan.: 31 days Jul.: 1 day
Sum	24 days	42 day	32 days
1998/99	Sep.: 10 days	0 days	Aug.: 3 days
Sum	10 days	0 days	3 days
1999/00	Feb.: 1 day	Jan.: 31 days	Jan.: 31 days Feb.: 1 days

Sum	1 days	31 days	32 days

The bar diagrams in figures II.1, II.2, II.3, II.4 show the data availability of the stations over the whole investigation periods.

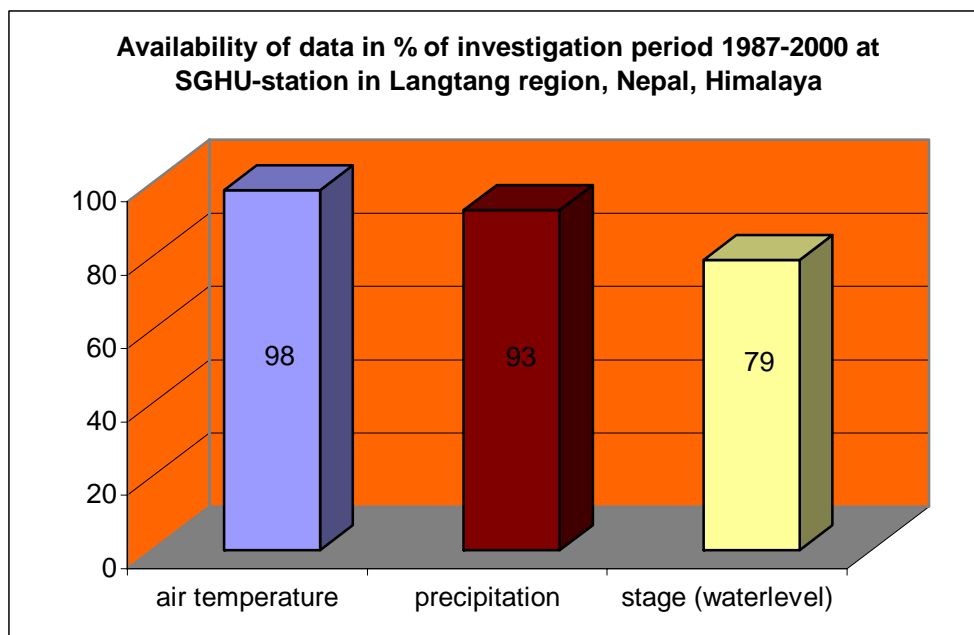


Fig. II.1: Availability of data in % of investigation period 1987-2000 at SGHU-station in Langtang region, Nepal, Himalaya.

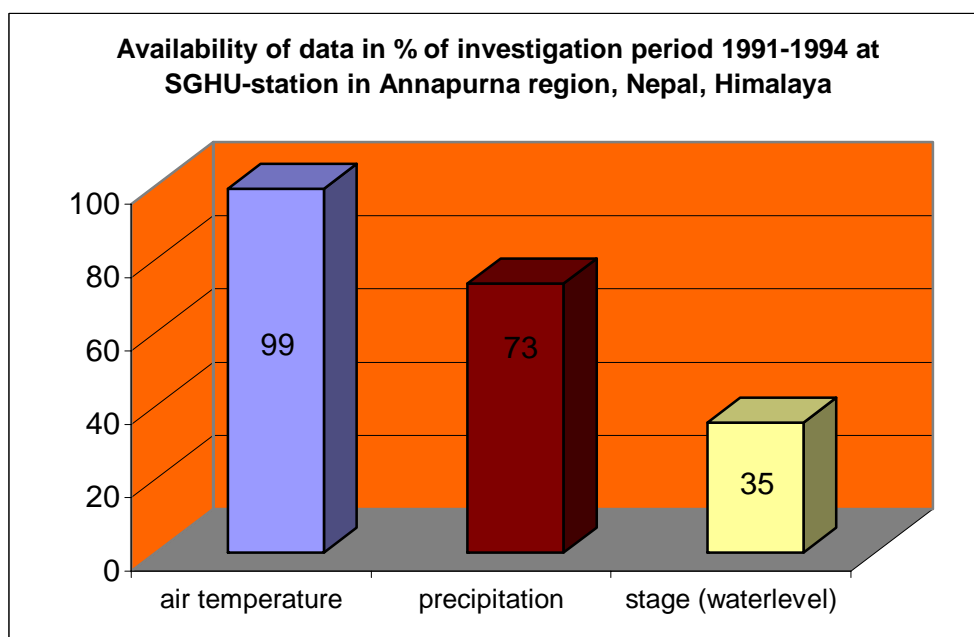


Fig. II.2: Availability of data in % of investigation period 1991-1992 at SGHU-station in Annapurna region, Nepal, Himalaya.

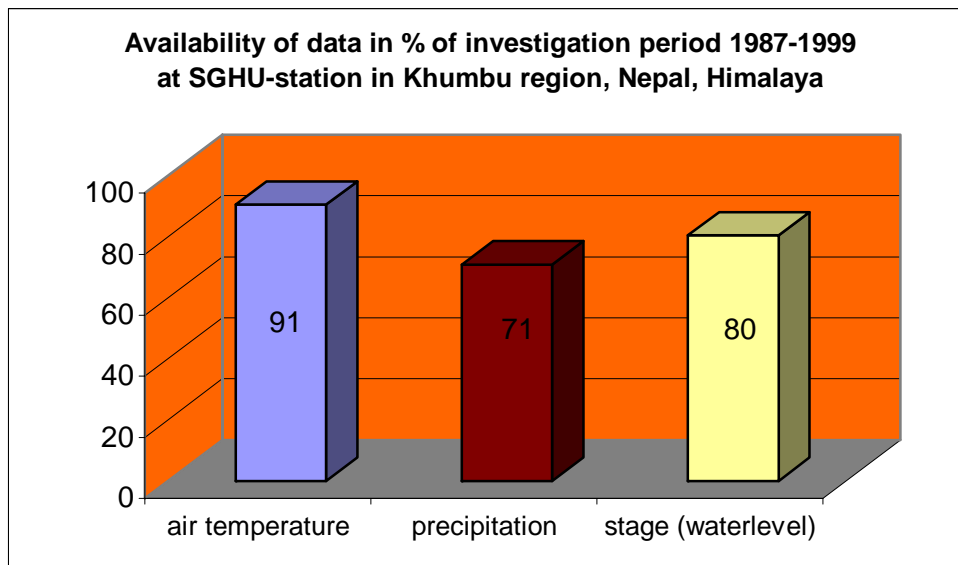


Fig. II.3: Availability of data in % of investigation period 1987-1999 at SGHU-station in Khumbu region, Nepal, Himalaya.

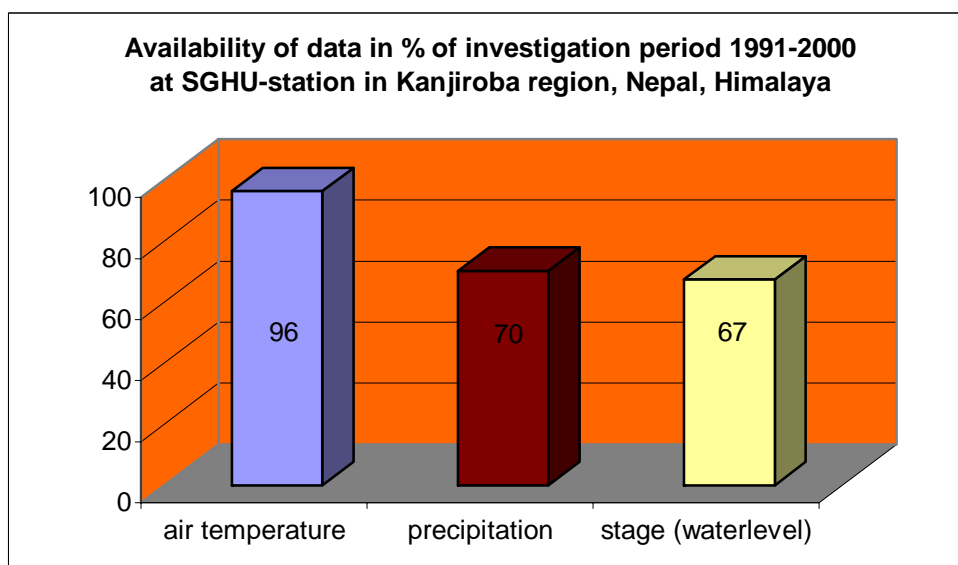


Fig. II.4: Availability of data in % of investigation period 1987-1999 at SGHU-station in Kanjiroba region, Nepal, Himalaya.

II.3 Rating curves

Discharge data are derived from gauge height using stage-flow calibration measurements executed by SGHU staff during their field trips around the year. Tracer dilution methods are used to measure discharge as described by Spreafico and Grabs (1993). For each investigation area specific rating curves are derived to calculate discharge out of gauge height. The following table II.5 contains the rating curves used to calculate discharge data. The R^2 -value judges the quality of the stage-flow relation.

Tab. II.5: Equations of rating curves of investigated catchments and corresponding R²-values

Catchment	Rating curve equation	R ² -value
Annapurna	$8.109 \cdot (\text{gauge height})^{2.039}$	0.98
Khumbu	$16.561 \cdot (\text{gauge height} + 0.076)^{2.364}$ *	0.99
Kanjiroba	$11.767 \cdot (\text{gauge height})^{1.5003}$	0.93
Langtang	$8.409 \cdot (\text{gauge height} - 0.078)^{1.334}$ *	-

* rating curve derived by SGHU

The availability of measured discharge values of Kanjiroba is very poor therefore the rating curve might be inaccurate.

II.4 Area Information

Area information are derived from digital elevation models based on the maps of the Survey Department. The HBV3-ETH9 model requires several area information like the distribution of the catchment area into exposition classes north, south and east-west-horizontal and into altitude belts. In this study altitude belts of 500 m are used (chapter I and IV). These information are calculated with the GIS software ArcView. The glacier covered area is taken from ICIMOD's glacier inventory 2002 (ICIMOD 2002).

Table II.6 shows the digital maps, which are used in the study.

Tab. II.6: Digital maps used to derive the area information for all catchments.

Catchment	Sheet No.	Date of aerial photography	Date of field verification	Scale
Langtang	2885 11	1992	1996	1:50,000
	2885 15	1992	1996	1:50,000
	2885 16	1992	1996	1:50,000
Annapurna	2883 08	1996	2000	1:50,000
Khumbu	2786 04	1992	1996	1:50,000
Kanjiroba	2982 11	1996	2001	1:50,000
	2982 12	1996	2001	1:50,000
	2982 15	1996	2001	1:50,000
	2982 16	1996	2001	1:50,000

The table contains the sheet No., date of aerial photography, date of field verification and the scale which is 1:50,000 at all maps. All maps are produced by the Survey Department of His Majesty's Government of Nepal in co-operation with the Government of Finland. The printed maps are similar to the digital maps.

In the case of Langtang catchment the digital maps of the Survey department do not cover the whole catchment area. The north-western part is located in China therefore the map of the German Alpine Club (DAV) is used to derive the area and glacier distribution of this part of the catchment. The following table II.7 gives the data of the additional DAV map called "Langthang Himal-Ost".

Tab. II.7: Additional map of Langtang catchment, which covers the Chinese part of the Langtang catchment.

Catchment	Sheet No.	Date of aerial photography	Date of field verification	Scale
Langtang	DAV 0/11	1973	-	1:50,000

The glacier distribution is derived from the digital maps of ICIMOD's glacier and glacier lake inventory in co-operation with UNEP (ICIMOD 2002).

Digital data sets of the Land Observation Satellite (LANDSAT)-5 Thematic Mapper (TM) and Indian Remote Sensing Satellite Series 1D (IRS1D) and Linear Imaging and Self Scanning Sensor (LISS)3 were used mostly for the inventory. Some data sets of Système Probatoire d'Observation de la Terre (SPOT) Multi-Spectral (XS) and SPOT Panchromatic (PAN) were also used.

The topographic maps used were published by the Survey of India in the period from the 1950s to the 1970s on a scale of 1 inch to 1 mile (i.e. 1:63,360) and by the Survey Department of His Majesty's Government of Nepal (HMGN) in 1996 on a scale of 1:50,000. The topographic maps of the Survey Department were based on aerial photographs from 1992 and field verification in 1996.

The aerial photographs (1:50,000 scale) used for ICIMOD's glacier inventory were taken in 1992 for eastern Nepal and in 1996 for western Nepal.

Prints of the satellite images in the form of planimetric maps on a scale of 1:250,000 published by the Remote Sensing Centre of Nepal in 1984 have been used for the inventory of glaciers and glacial lakes. Landsat MSS data in digital format from March–April 1994, resampled in 50m pixel size, are available at ICIMOD.

These information are taken from the free available CDROM "Inventory of glaciers, glacier lakes and glacier lake outburst floods monitoring and early warning systems in the Hindu Kush – Himalayan region" of ICIMOD in co-operation with UNEP.

II.5 Reference stations

For the bridging of data gaps (chapter III) stations of the Standard Data Meteorological Service Network of DHM were used. The following table II.8 shows a summary of stations with elevation and station code.

Tab. II.8: Summary of DHM reference stations used for data processing.

Region	Station	Elevation	Measurements	Code
Kanjiroba	Jumla	2300	TP	303
Humla	Gam Shree Nagar	2133	P	306
Humla	Rara	3048	TP	307
Kanjiroba	Dunai	2058	TP	312
Humla	Darma	1950	P	313
Annapurna	Pokhara Airport	827	TP	804
Annapurna	Malepatan (Pokhara)	856	TP	811
Annapurna	Bhadaure Deurali	1600	P	813
Annapurna	Lumle	1642	TP	814
Annapurna	Lamachaur	1070	P	818
Annapurna	Ghandruk	1960	P	821

Annapurna	Siklesh	1820	P	824
Langtang	Timure	1900	P	1001
Langtang	Sarmathang	2625	P	1016
Langtang	Kathmandu Airport	1336	TP	1030
Langtang	Thamachit	1847	P	1054
Langtang	Dhunche	1982	TP	1055
Langtang	Tarke Ghyang	2480	P	1058
Langtang	Paigutary	????	TP	1072
Khumbu	Chaurikharka	2619	P	1202
Khumbu	Pakarnas	1982	P	1203
Khumbu	Aisealukhark	2143	P	1204
Khumbu	Okhaldhunga	1720	TP	1206
Khumbu	Khumjung	3750	P	1217
Khumbu	Salleri	2378	P	1219
Khumbu	Chialsa	2770	TP	1220

CHAPTER III DATA PROCESSING

III.1 Bridging of data gabs

As shown in chapter II the data have a lot of gabs either in precipitation and temperature data or in runoff data. Due to the integral structure of the algorithm of the HBV3-ETH9 model it is important to get complete input data of precipitation and temperature. Therefore the gabs in precipitation and temperature have to be bridged with useful methods. To derive reliable data basis extrapolation methods were used as described in Weber 1997 with few extensions in the extrapolation of precipitation data. The procedure combines the long-term data series of the standard meteorological stations at low altitudes with the relatively short data series from high mountain stations to bridge gabs in the data series of the catchment records. Due to an analysis of monthly air temperature gradients a statistical method was found which takes into account the differences in the stratification of the lower atmosphere in the lowlands (generally well-mixed) and higher mountain regions (generally neutral or stable). Bridging of data gabs in the precipitation series of SGHU stations is necessary if observations are missing or instead of daily readings only sums over several days are recorded here the sums have to be redistributed over the individual days. Following steps were taken to derive precipitation data to fill the gabs:

- a. determination of the occurrence probability of precipitation for each station for each month;
- b. determination of the joint probability of precipitation occurrence at the SGHU station and the DHM reference stations;
- c. determination of the mean ratio of monthly sums of precipitation at the SGHU station and the DHM reference stations;
- d. determination or estimation of the "true" monthly sums of precipitation at the SGHU station.

These procedures were used for Langtang, Annapurna, Khumbu and Kanjiroba catchments and are described in the next sub-chapters.

III.2 Extrapolation of air-temperature data

III.2.1 General remarks

The current value of air-temperature (generally 2m above ground) is not only depending on the entire synoptic situation and the altitude but also on local vertical and horizontal exchange conditions. Horizontal processes can be all advective processes like local wind systems or frontal passages, vertical distribution of air-temperature is determined by the surface energy balance. There are further processes in orographic heavily subdivided areas. Therefore air-temperature is heated up stronger in narrow mountain valleys than in flat areas, due to the energy input of the sensible heat flux. On the one hand the energy is distributed to a larger air volume and on the other hand the heating area is bigger in the valleys. There is a stronger cooling during radiation free time (e.g. night) because of the ratio of

reflecting area and air volume. Additionally there are cold air seas because of the density of cold air.

An other important effect is the composition of the ground. Great impacts are given by the reflection, head conductivity of soil, water content and vegetation as well as the roughness of spoil. The roughness of spoil impacts the turbulence and therefore the exchange of radiation in the terms of the energy balance. The other values are responsible for the division of the terms of the energy balance.

The mentioned impacts on local air-temperature measurements are not complete but it can be clarified that even in a small area temperature measurements at different stations cannot be easily transferred from one station to the other. As an example for this theory annual temperature graphs of different stations in Khumbu region are shown in figure III.1.

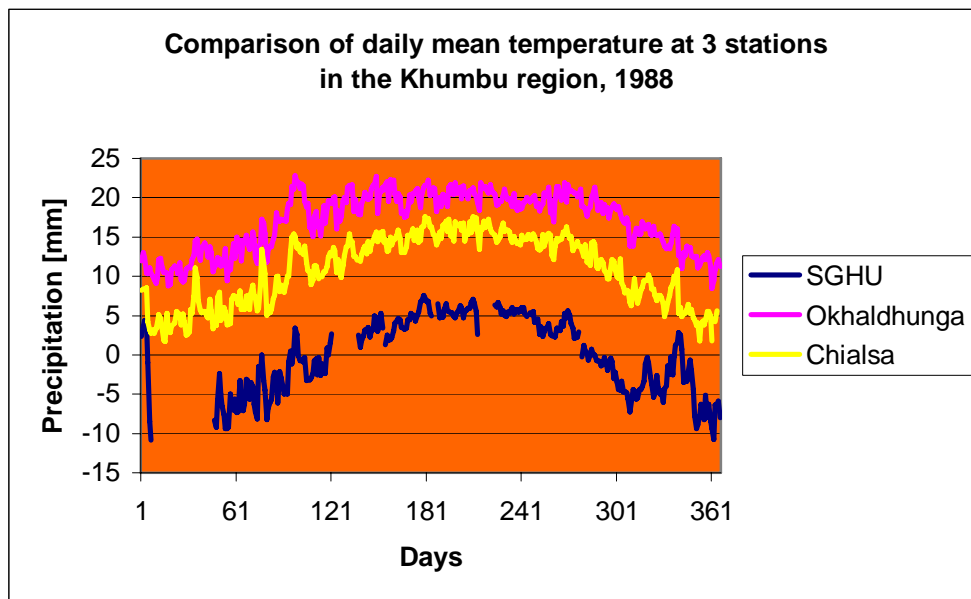


Fig. III.1: Comparison of graphs of temperature at three climatological stations Okhaldunga (1720m), Chialsa (2770m) and Dingboche (SGHU Station, 4355m) in Khumbu region, 1988.

The most important impact on temperature is given by the sea-level of the climatological station. An increasing variation of the data series can be stated with increasing altitude which might be an indicator for the rough climate in the higher regions. There is also a typical higher variation during dry season than during monsoon season at higher stations.

Figure III.2 shows the correlation of the same stations in Khumbu region with the SGHU station in 1988.

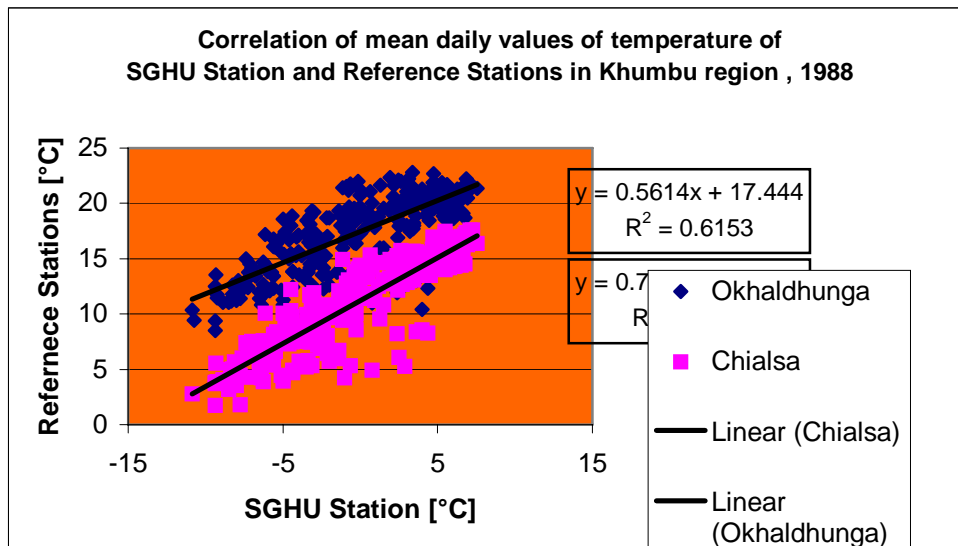


Fig. III.2: Correlation of daily mean values of temperature of Okhaldhunga (1720m), Chialsa (2770m) and Dingboche (SGHU Station, 4355m) in Khumbu region, 1988.

The linear regression shows that no station fits good to the SGHU station. To bridge data gaps the simple linear regression is not a useful method as the R^2 values of 0.61 and 0.79 shows. An other method must be found to derive synthetic time series. The R^2 values change from region to region depending on the position of reference station to the SGHU station.

III.2.2 Procedure of extrapolation of daily mean air-temperature values

For the extrapolation of temperature values an universal regression method is useful, analogue to the linear regression, which depends only on temperature values of the reference stations. Results with sufficient accuracy were achieved with following function:

$$T_{\text{SGHU}} = A \cdot T_{\text{Ref}}^2 + B \cdot T_{\text{Ref}} + C \quad (\text{III.1})$$

A,B,C: coefficients
 T_{SGHU} : Temperature at SGHU station
 T_{Ref} : Temperature at reference station

The coefficients A,B,C are determined from mean monthly temperature values regressively as shown in figure III.3.

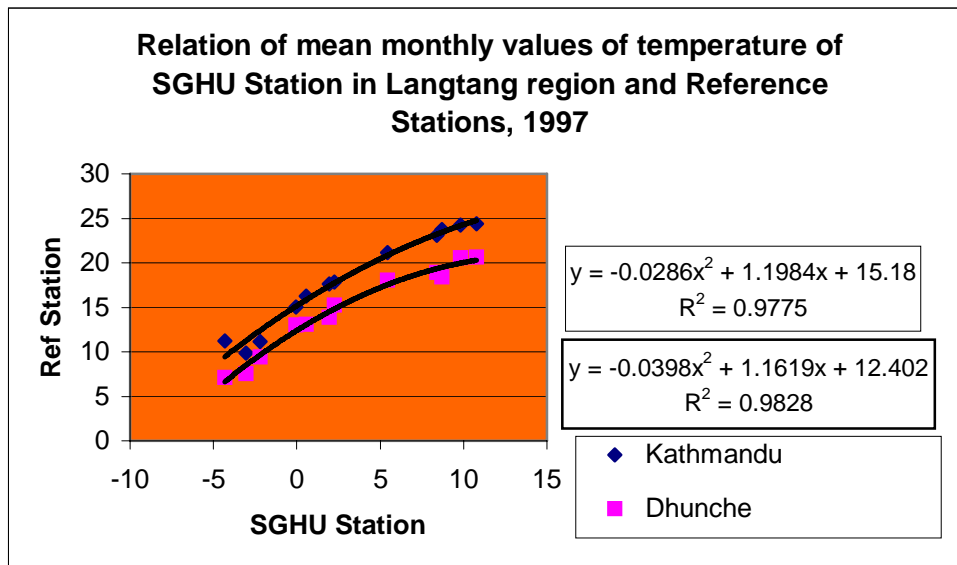


Fig. III.3: Empirical relation between reference stations and SGHU station with a second-order polynomial function.

The value C gives approximately the mean annual temperature difference between the stations. The B value should be near 1. A describes mainly the impact of atmospheric stratification. The coefficients were determined for the catchments where enough data were available. Figure III.3 shows the equations for the stations in Langtang region and the corresponding R²-values which are much better than the R²-values of the corresponding linear regression.

The comparison of measured and calculated temperature values, as shown in figure III.4, looks quit good. Even single structures are modelled realistically and the increasing amplitude of variation during dry season are hit well.

The objective visualisation of quality control, shown as relation of measured and calculated values in figure III.5, clarifies that the parameter of the linear regression deviate from a proper 1:1 relation and failures of several degrees have to be taken into account. In reality the situation of air-temperature data is not that bed and there is no need to use the complete synthetic time series. Only small gabs of several days or a month have to be bridged for which the extrapolation method delivers an objective suggestion and can be used as a "First Guess".

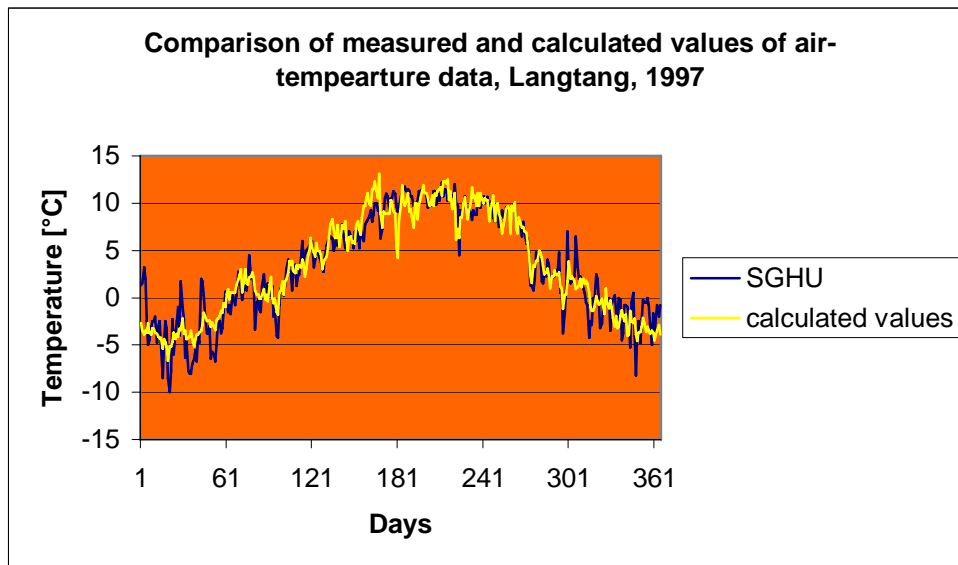


Fig. III.4: Comparison of measured values and calculated values of air-temperature in Langtang region, 1997.

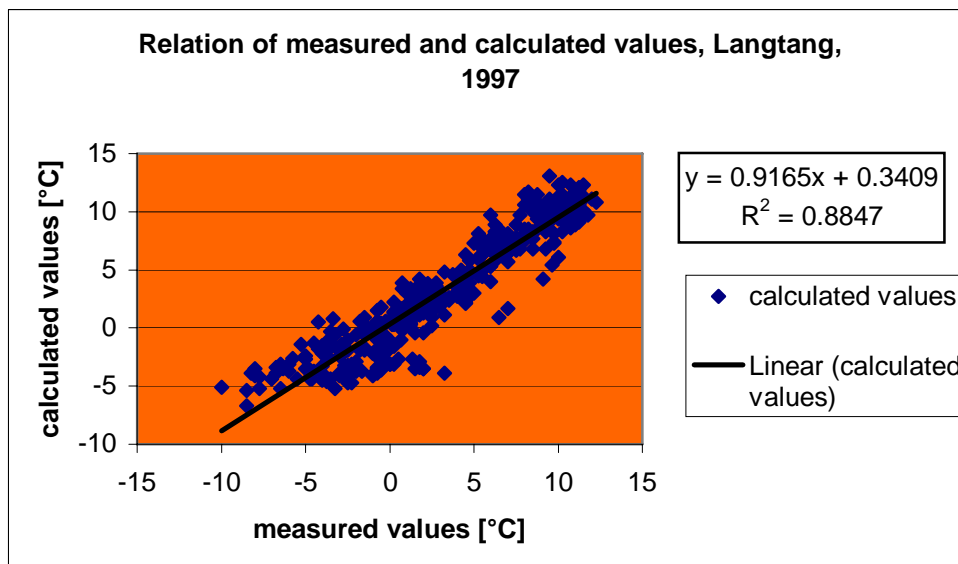


Fig. III.5: visualisation of quality control shows a fit of 88 % between measured and calculated values for Langtang region, 1997.

An example of the procedure of data extrapolation is visualised in figure III.6. The development of the modified time series is defined by the extrapolated values and by the original measured values which reduces the failures. The failures are not zero but should be below 1 K in most cases (Weber 1997). The gaps in air-temperature time series can be bridged with this method with an accuracy which is sufficient to create complete time series which is important for HBV3-ETH9 modulation. Modulation results have shown that this quit simple method is exact enough to bridge data gaps and to create complete time series of air-temperature data.

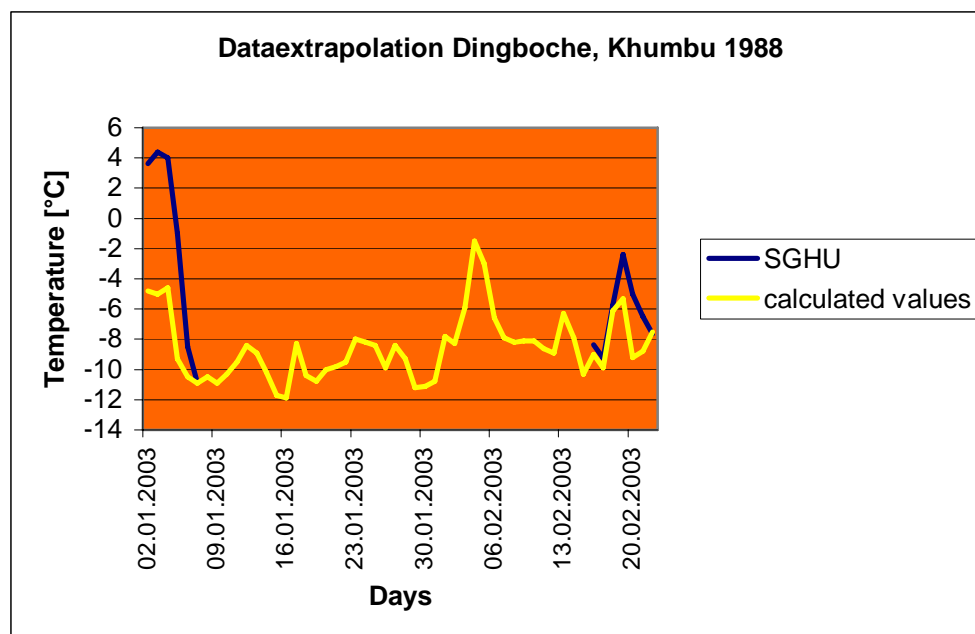


Fig. III.6: Example for the procedure of data bridging with the help of measured and calculated values of air-temperature of Khumbu region, 1988.

III.3 Extrapolation of precipitation data

III.3.1 General remarks

Nepal's precipitation is of a continental type and predominantly convective. There are distinctive dry seasons and rainy seasons and precipitation events are short but very intensive. In dry season precipitation is quite rare as well as days without precipitation in rainy season. This characteristic enables an approach to reconstruct daily values of precipitation at a SGHU station with adequate reliability.

In the case of runoff modelling with HBV3-ETH9 it is important to get nearly realistic precipitation data in daily dissolution. If precipitation is solid it will be assigned to storage and contributes to run maybe weeks or months later. Therefore it is more important to get the total amount of snowfall then the realistic distribution of snow to the corresponding days. Stricter rules must be set in case of rainfall. If storages are filled, liquid precipitation contributes to runoff directly therefore it is important to get a realistic distribution of rain to the corresponding days.

The HBV3-ETH9 model contains a lot of parameter which are important for runoff calculation and the exact assignment of amount and time of precipitation is only one factor. More important for runoff calculation is the temporal correct determination of melt water production, which is however directly related to temperature. Nevertheless it is important to derive realistic data series of precipitation to simulate short time fluctuation in runoff. The filling of data gabs is necessary if observations are missing or instead of daily readings only sums over several days are recorded.

III.3.2 Procedure of extrapolation of daily sums of precipitation

The procedure of extrapolation of daily sums of precipitation is a statistical based method, developed by Weber 1997, which takes different reference stations of the corresponding region into account. With the help of the cluster of reference stations

event probability and amount of precipitation at the target station (SGHU stations) can be derived.

The complete data will be analysed after following criteria:

- a. determination of the occurrence probability of precipitation for each station for each month;
- b. determination of the joint probability of precipitation occurrence at the SGHU station and the DHM reference stations;
- c. determination of the mean ratio of monthly sums of precipitation at the SGHU station and the DHM reference stations;
- d. determination or estimation of the "true" monthly sums of precipitation at the SGHU station.

The criteria of a. is the amount of days per month with precipitation > 1mm. For b. the amount precipitation or precipitation free days at SGHU and reference stations is deciding. The ratio of c. delivers a dimension of the amount of precipitation which can be expected during a precipitation event at the target station (SGHU station). In high alpine regions an increasing amount of precipitation with altitude like in lowlands is not necessary. Local wind effects are more important and the theoretically possible amount of precipitation cannot increase with altitude due to the declining water holding capacity of air because of decreasing air-temperature. Therefore the potential amount of precipitation at high alpine stations is lower than at low land stations. The value of d. is used to match the synthetic precipitation data to a more realistic value. This point is quite delicate because of data gaps in SGHU time series. If no data is available this value must be guessed intuitively.

The daily amount of precipitation P_s will be calculated on the basis of this information with following equation.

$$P_s = 1/N \cdot K_m \cdot S (P_i \cdot F_{i,m} \cdot W_{i,m}) \quad (III.2)$$

P_i is the measured precipitation at reference station i , $F_{i,m}$ mean ratio of amount of precipitation between station i in the month m and target station (SGHU station), $W_{i,m}$ is the weighting of station i in ratio to the occurrence probability of precipitation. K_m is a correction factor for the probabilities. P_s has to be matched to the current monthly sums at target station.

With table III.1 the matrix of mean ratio of sums of precipitation between reference stations and SGHU station can be derived. Table III.2 shows the $F_{i,m}$ values of equation (III.2).

Figure III.7 shows mean daily occurrence probabilities of precipitation in Annapurna region. The occurrence probability is given in %. It can also be interpreted as percentage amount of days with precipitation per month. As an example it is raining nearly every day in Lumle in July and August while Pokhara has only at 22 of 31 days rain. Bhadaure-Deurali is in the south of Lumle and in a downwind exposition therefore precipitation probability is lower. Lumle has the most precipitation days. At SGHU station even in April there is precipitation nearly every day.

Figure III.8 demonstrates the probability of corresponding occurrence of precipitation events at the Machapuchhre B.C. station (SGHU station) and a lowland stations situated in the Annapurna region.

Tab. III.1: Mean monthly sums of precipitation in Annapurna region, 1991-1994 mean annual sums and mean annual ratio of amounts to SGHU station. Boltic values are not statistically protected. Red values are estimated values.

month	SGHU	Ghandruk	Lumle	Bhadaure D.	Lamachaur	Siklesh	Pokhara	Malepatan
1	43	16	40	20	26	49	17	22
2	87	49	47	10	34	61	29	38
3	136	25	56	15	13	46	45	43
4	336	44	86	30		122	96	132
5	90	135	305	312	621	269	336	401
6	203	511	786	564		472	576	526
7	236	610	1163	705	1234	572	894	983
8	321	1080	1500	878		857	841	976
9	147	369	911	693		427	638	646
10	28	27	183	118		92	174	212
11	8	23	20	12	0	20	3	6
12	29	20	18	12	6	27	15	11
year	1664	2909	5115	3369	1934	3014	3664	3996
factor		0.5720	0.3253	0.4939	0.8604	0.5521	0.4541	0.4164
altitude	3470	1960	1642	1600	1070	1820	827	856

Tab. 2: Mean monthly ratio of precipitation sums between SGHU station Machapuchhare B.C. and reverence stations derived with data of table 1. Boltic values are derived from estimated values.

month	SGHU	Ghandruk	Lumle	Bhadaure D.	Lamachaur	Siklesh	Pokhara	Malepatan
1	1.000	2.688	1.075	2.150	1.654	0.878	2.529	1.955
2	1.000	1.776	1.851	8.700	2.559	1.426	3.000	2.289
3	1.000	5.440	2.429	9.067	10.462	2.957	3.022	3.163
4	1.000	7.636	3.907	11.200	5.000	2.754	3.500	2.545
5	1.000	0.667	0.295	0.288	0.145	0.335	0.268	0.224
6	1.000	0.397	0.258	0.360	0.210	0.430	0.352	0.386
7	1.000	0.387	0.203	0.335	0.191	0.413	0.264	0.240
8	1.000	0.297	0.214	0.366	0.210	0.375	0.382	0.329
9	1.000	0.398	0.161	0.212	0.150	0.344	0.230	0.228
10	1.000	1.037	0.153	0.237	0.150	0.304	0.161	0.132
11	1.000	0.348	0.400	0.667	1.000	0.400	2.667	1.333
12	1.000	1.450	1.611	2.417	4.833	1.074	1.933	2.636

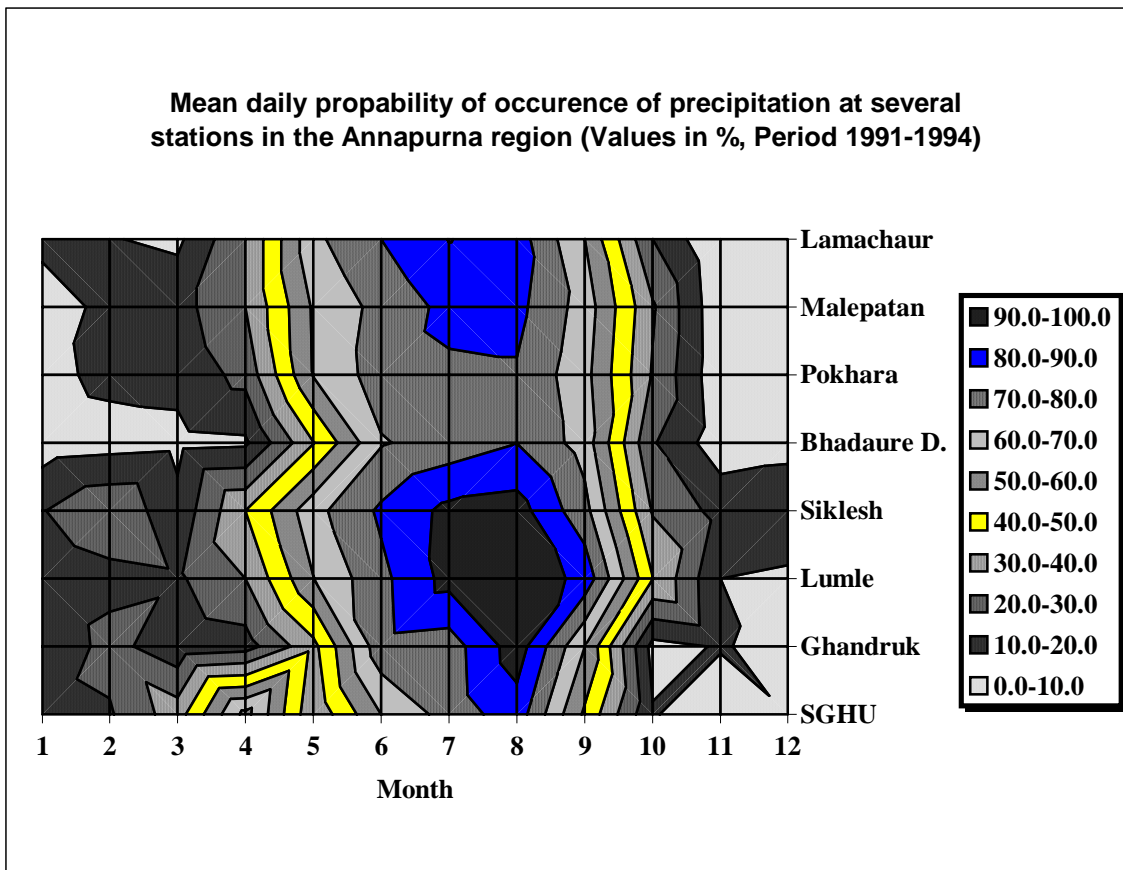


Fig. III.7: Probability of occurrence of precipitation in Annapurna region. Source Weber (1997).

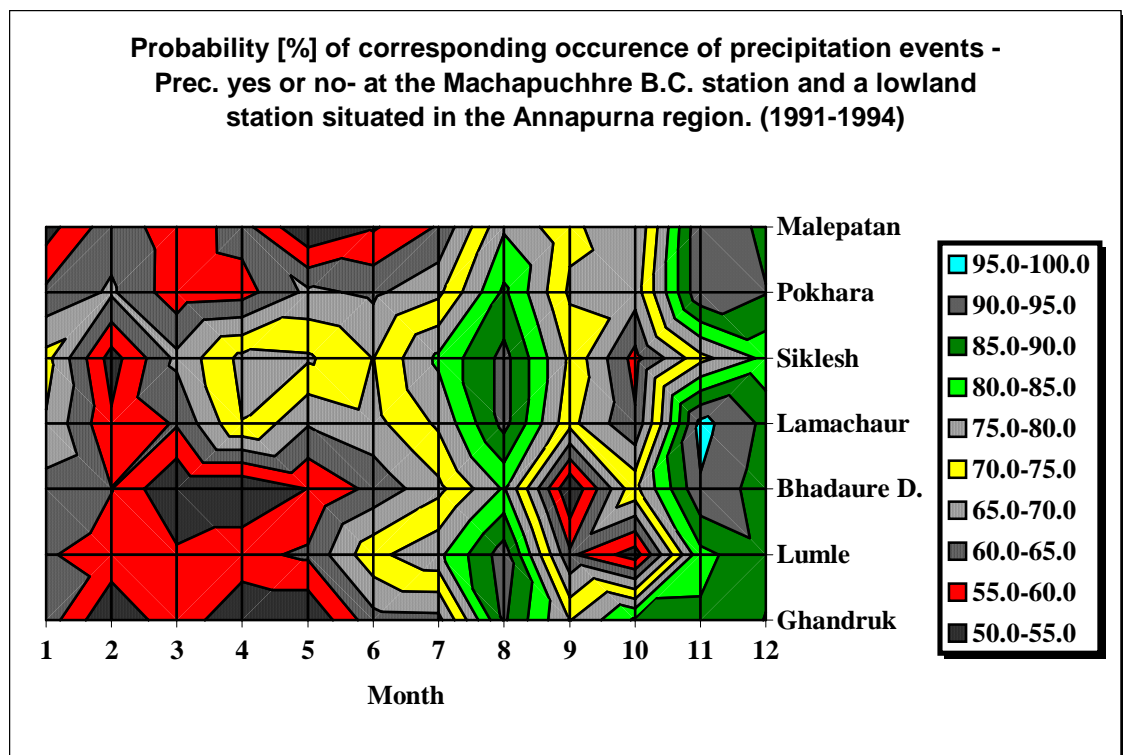


Fig. III.8: corresponding occurrence of precipitation events at the SGHU station and a lowland stations situated in the Annapurna region. Source Weber (1997).

With all these information synthetic daily sums of precipitation can be calculated. The algorithm over estimates the real sums of precipitation so a adequate method to adjust the synthetic values to reality has to be found. Therefore the mean ratio of monthly sums of precipitation of extrapolated values and measured values of month without gabs is calculated and taken as a transformation value, as shown in table III.3, to adjust the synthetic data. Figures III.9 and III.10 point out an example of the procedure of the adjustment of synthetic data to more realistic data in the case of data gabs over a whole month.

Tab. III.3: Calculated and measured monthly sums of precipitation of years without gabs in March, SGHU station in Langtang region.

year	Extrap.	Org.	Quotient	Mean quotient
1988	130.7	56.2	2.3	2.6
1989	81.7	31	2.6	
1992	47.1	14	3.4	
1993	50.3	27.4	1.8	
1994	50.5	13.2	3.8	
1997	37	21.5	1.7	
1998	184.5	40.8	4.5	
1999	5	21.8	0.2	

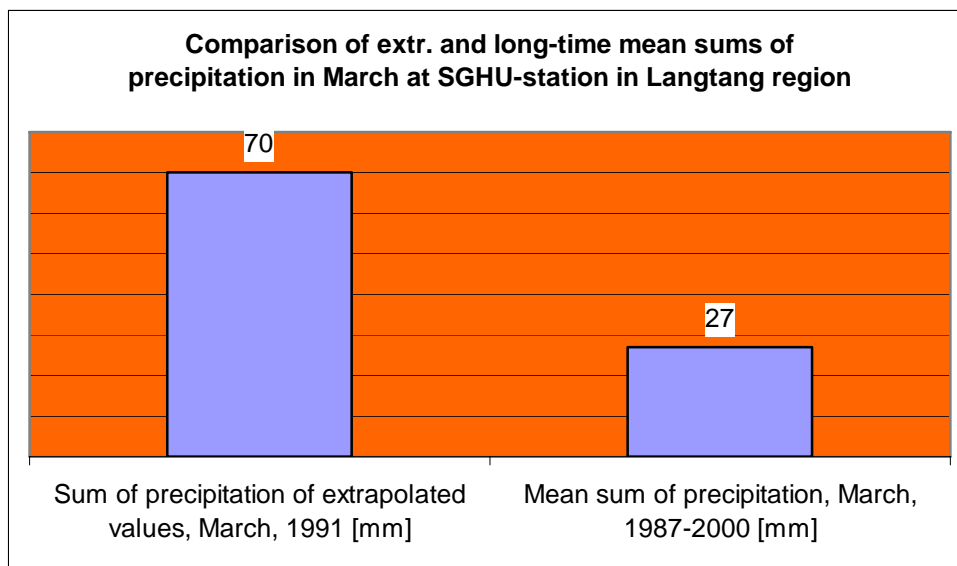


Fig. III.9: Comparison of extrapolated and long-time mean sums of precipitation of March at SGHU station in Langtang region.

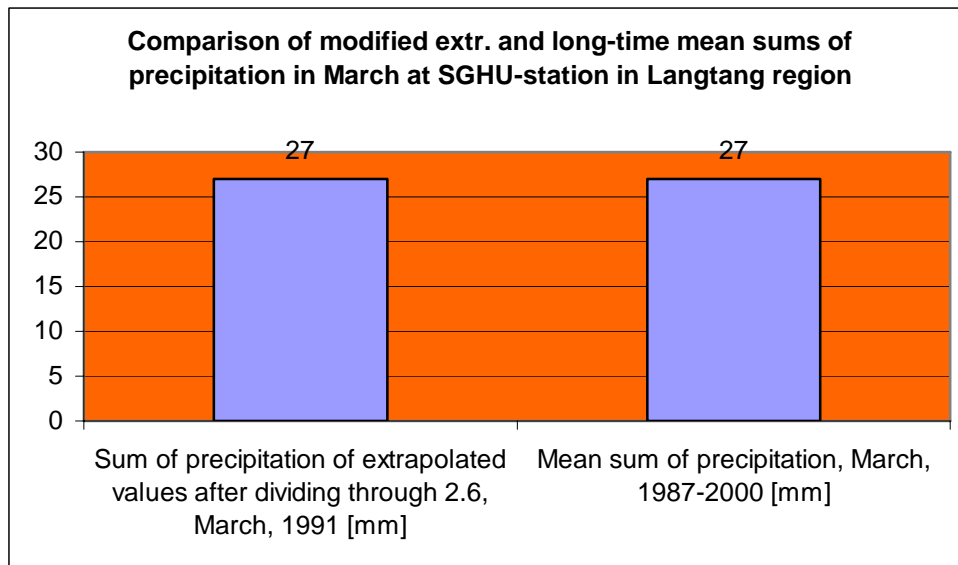


Fig. III.10: Comparison of modified extrapolated and long-time mean sums of precipitation in March at SGHU station in Langtang region.

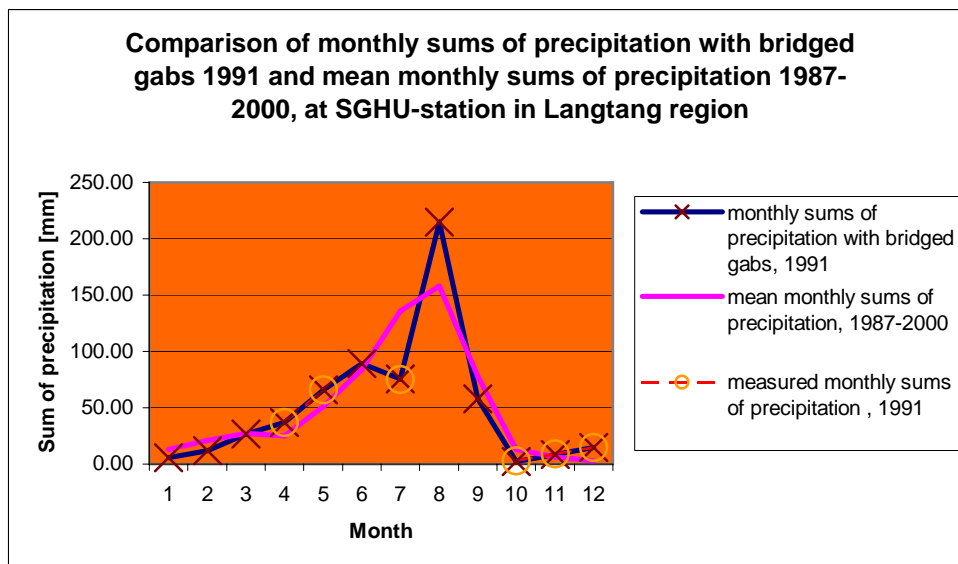


Fig. III.11: Comparison of monthly sums of precipitation with bridged gabs 1991 and mean monthly sums of precipitation 1987-2000, at SGHU station in Langtang region.

Figure III.11 shows an example of the whole procedure of data processing and bridging of gabs in precipitation series. If there are measured values available they are used and only gabs are bridged with the help of synthetic values. Therefore the reliability of the complete data series is more reliable than the synthetic time series. An additional subjective criterion to check the reliability of the transformation value is a statistic over the percentage deviation of monthly sums of precipitation of SGHU and reference stations from long-time mean values. These percentage values show whether the month is wetter or dryer than the long-time mean. In the example of March 1991 at SGHU station in Langtang region table III.4 shows some stations which are wetter (stations 1001, 1055) than the long-time mean and others which are dryer (1058, 1016). March 1991 is a month without special trends like dryer or wetter. An example for an dryer month is October 1991 where all stations show a negative trend. Therefore the transformation value (2.6) seems to be quite reliable

because it delivers a modified extrapolated sum of 27 mm which is exactly the same as the long-time value of March (figure III.10). This criterion is only subjective but it gives some support to judge the transformation values.

Tab. III.4: Deviation of monthly sums of precipitation from long-time mean of precipitation in 1991 at SGHU station and reference stations in Langtang region.

month	SGHU	1001	1054	1072	1055	1058	1016	1030
1			0	-100		-12	25	31
2			83	-100	-18		-83	-42
3		102		-100	2	-47	-97	32
4	48		-33	-100	-32	-26	-97	89
5	29	13		-11			-69	
6		42		71			-84	
7	-45		-31	40		-22	-94	-49
8			-3	37		-14	-62	-11
9				8		3	-45	
10	-77	-93	-60	-100			-64	-100
11	50	-57	-100	233			-89	-100
12	400	0	100	92		38		56

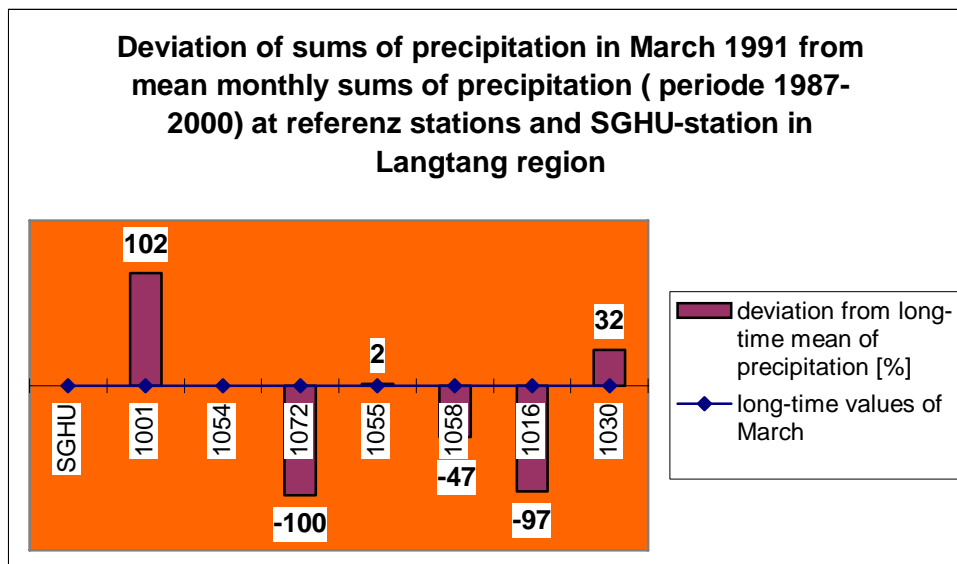


Fig. III.12: Deviation of sums of precipitation in March 1991 from mean monthly sums of precipitation (period 1987-2000) at referenz stations and SGHU station in Langtang region.

Figure III.13 shows the mode of operation of the extrapolation algorithm in the case of cumulated values in the original data series of SGHU station in Annapurna. The cumulated value at 11th June must be redistributed over the previous days and the extrapolated value has to be adjusted to a more realistic value. Figure III.14 shows how the algorithm works here. With 97.2 mm the modified extrapolated value hits the cumulated value of 100.3 mm quite good and the amount of precipitation is redistributed over the previous eleven days which is much more reliable than the cumulated value of 100.3 mm.

Figure III.15 shows an example, which is statistically more sufficient. The comparison between the original daily sums of precipitation recorded at Machapuchhre B.C. station, Annapurna, and those extrapolated from the data of

several climatological stations, 1991. Reliable values of precipitation are taken unchanged to the extrapolated values. The new data series does not represent 100% realistic values but delivers a data series of high probability and plausibility.

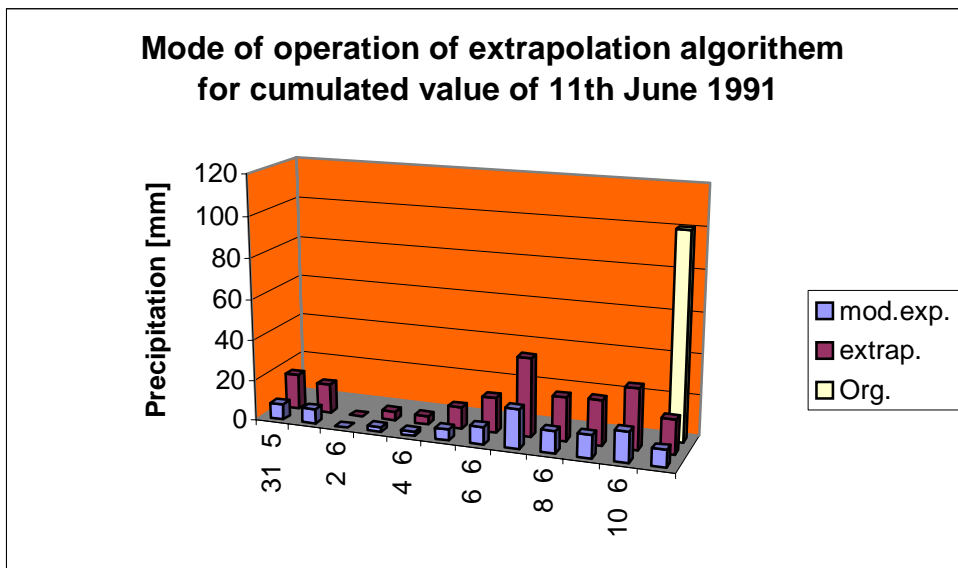


Fig. III.13: Mode of operation of extrapolation algorithm for redistribution of cumulated value of 11th June 1991, SGHU station Annapurna.

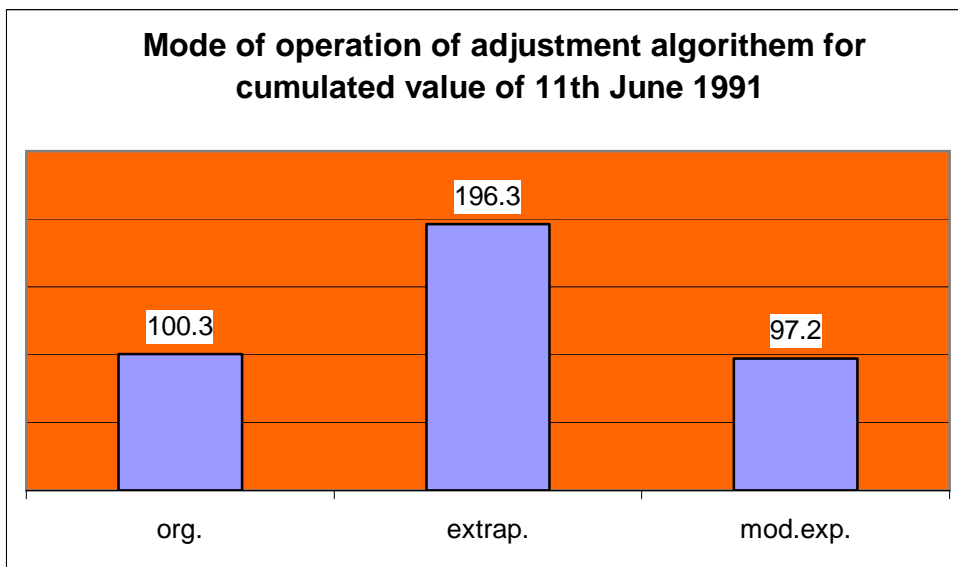


Fig. III.14: Mode of operation of extrapolation algorithm for adjustment of extrapolated value to a more realistic value, 11th June 1991, SGHU station Annapurna.

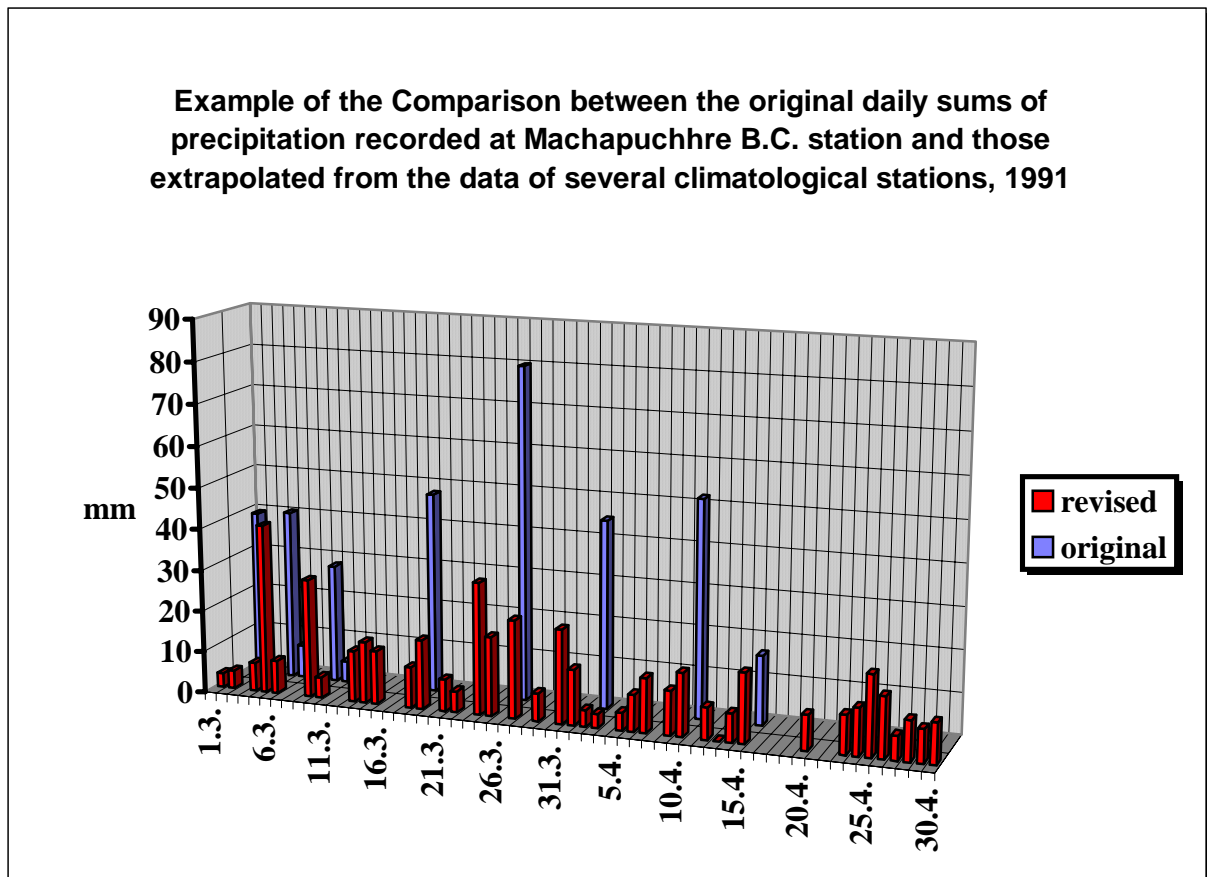


Fig. III.15: Mode of operation of extrapolation algorithm for redistribution of cumulated value of a longer period in 1991, SGHU station Annapurna. Source Weber (1997).

CHAPTER IV THE HBV3-ETH9 MODEL

IV.1. Structure of HBV3-ETH9

The HBV3-ETH9 precipitation-runoff model is a further developed version of the widely used HBV model with special features to calculate the runoff of alpine catchments. The HBV model was developed in 1973 at the Swedish SMHI (Swedish Meteorological and Hydrological Institute) and was developed further at the ETH Zurich (Bergström 1992; Braun und Renner 1992; Hotteliet et al. 1993). This conceptual model considers all important components of water balance. The component connection is realised by parameters which have to be calibrated for each catchment. This chapter contains a detailed description of the construction of HBV3-ETH9 and an explanation of all important parameters to run the model.

The model describes hydrological processes with simplified and combined physical formulas. Therefore, it is a grey model which is placed between the white and the black-box model (e.g. unit-hydrograph). The great advantage of this concept is that the runoff can be calculated with only temperature and precipitation data, both of which can be measured easily. A good fit of calculated and measured runoff is

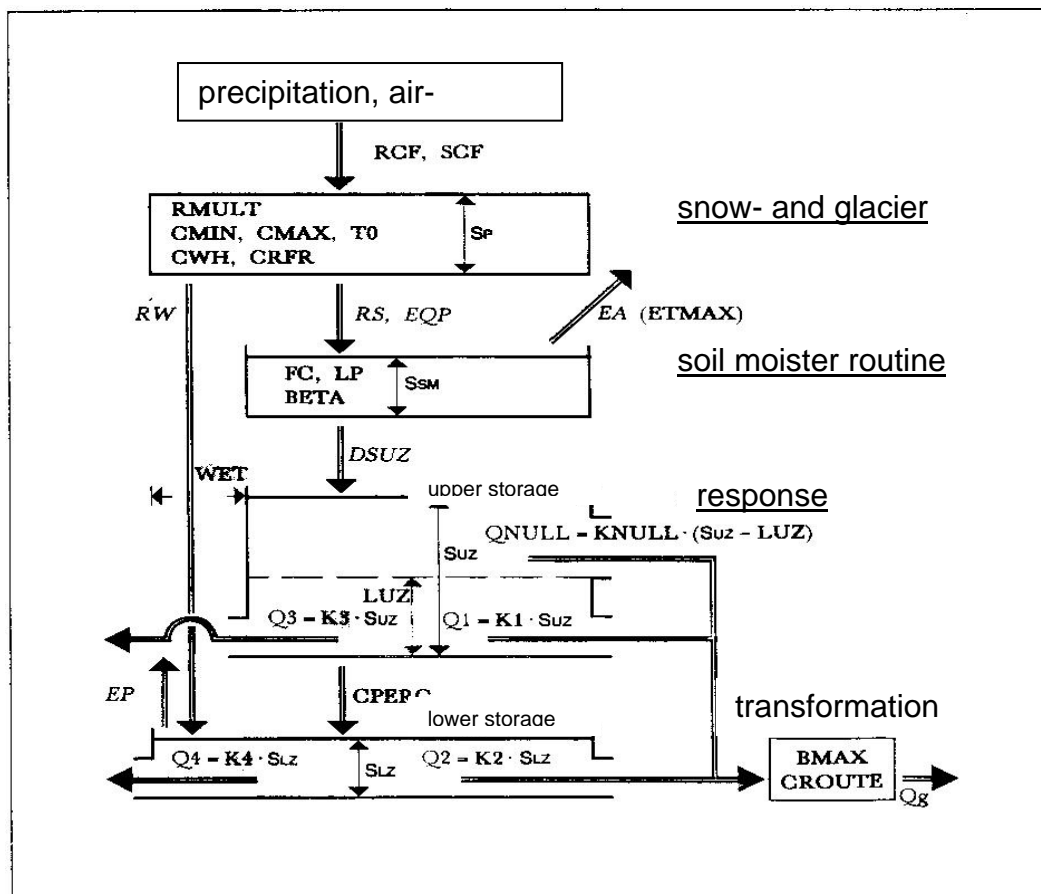


Fig. IV.1: Schematic view of the HBV3-ETH9 precipitation-runoff model (Hotteliet 1991).

achieved if there is a good calibration of the parameters. Illustration IV.1 shows a simplified diagram of the precipitation-runoff model which expresses the most important parameters and their affiliation to each function of the model.

The HBV3-ETH9 model is subdivided into three parts:

- snow- and glacier routine
- soil moisture routine
- response function

IV.2 Parameters of HBV3-ETH9

The model uses different kinds of parameters, parameters which are calculated in the model and represent the system statuses and processes (table IV.1) and parameters which can be optimized in the calibration procedure (table IV.2).

Tab. IV.1: Parameters which are calculated in the model and represent the system statuses and processes.

Parameter	Description of parameter	Unit
DSUZ	Influx into upper storage	mm
EA	Actual evaporation	mm/d
Q1	interflow, upper storage	mm/d
Q2	baseflow, lower storage	mm/d
QNULL	overlandflow, upper storage	mm/d
RS	Effective precipitation	mm
SLZ	Lower zone storage	mm
SSM	Soil moisture storage	mm
SUZ	Upper zone storage	mm

Tab. IV.2: Parameters which can be optimized in the calibration procedure.

Parameter	Description of parameter	Unit
BETA	Empirical coefficient controlling the outflow from soil moisture	$0 < \text{BETA} < \infty$
CMAX	Maximum of degree-day factor	mm/d °C
CMIN	Minimum of degree-day factor	mm/d °C
CPERC	Percolation capacity into lower zone	mm/d
CRFR	Refreezing coefficient	-
CROUTE	Parameter of transformation function	0 or 1
CWH	Retention, coefficient of water holding capacity	-
ETMAX	Maximum of evapotranspiration	mm/d
FC	Maximum soil moisture storage, field capacity	mm
K0	Storage discharge constants, upper zone	-
K1	Storage discharge constants, upper zone	-
K2	Storage discharge constants, lower zone	-
LP	Upper limit of potential evapotranspiration	mm
LUZ	Limit for fast drainage, upper zone	mm
PGRAD	Precipitation gradient	mm/100m
RCF	Rain correction coefficient	-
REXP	Increasing of snow-, ice melt depending on orientation of the slope	-
RMULT	Increasing melt of ice against snow	-
SCF	Snow correction coefficient	-
T0	Threshold value for transition of rain/snow and	°C

	calculation of snowmelt	
TGRAD	Temperature gradient	°C/100m

IV.3 Snow and glacier routine

The HBV3-ETH9-model uses an index method to calculate the snowmelt. Input data are only temperature and precipitation. The output is the effective precipitation RS, consisting of liquid precipitation and water of snowmelt. RS is the input into the soil moisture routine.

The following questions are considered:

- a.) Differentiation between liquid and solid precipitation.
- b.) Correction of measured precipitation for the compensation of
 - unsatisfactory representativeness of the measurement station
 - measuring errors for liquid and solid precipitation
- c.) Estimation of snowmelt
- d.) Estimation of intensity of orientation depending on ablation of snow cover
- e.) Estimation of storage and refreezing of liquid water in snow cover.

IV.3.1 Differentiation between liquid and solid precipitation

The mean daily air temperature measured at a representative station in the catchment is an input. It must be possible to deduce representative temperature developments of all altitudes of the catchment. Special meteorological situations such as inversions cannot be taken into account, and therefore catchments with many of these special meteorological situations will produce unsatisfactory results. Additionally, there is a T₀ parameter to extend the whole temperature level. If T_m is below the threshold value T₀, the precipitation on ground RS is considered to be accumulation of snow cover for this altitude. T₀ is an empirical coefficient and has to be determined for each catchment.

The linear affiliation of altitude and temperature is determined by TGRAD, which is the adiabatic gradient [K/100m] and which is seasonally constant for the catchment.

IV.3.2 Correction of measured precipitation for the compensation of

- **unsatisfactory representativity of the measurement station**
- **measuring errors for liquid and solid precipitation**

The sum of precipitation in a day, measured at single stations, is extrapolated over the whole catchment with the help of the parameters RCF (for rain) and SCF (for snow).

Systematic errors, like unsatisfactory representativity of the measurement station or measuring errors for liquid and solid precipitation, can be corrected with the help of precipitation correction coefficients.

The following simplified formulas are applied to improve precipitation data:

$$\Delta S_s = P \cdot SCF \text{ (air temperature} < T_0 \text{) (IV.1)}$$

$$P_{liq} = P \cdot RCF \text{ (air temperature } > T_0) \text{ (IV.2)}$$

ΔS_s = solid precipitation

P_{liq} = liquid precipitation

Furthermore, it is possible to use a precipitation gradient, PGRAD, to simulate the affiliation of the amount of precipitation with the altitude if there is a homogeneous distribution of precipitation over the whole catchment.

IV.3.3 Estimation of snowmelt

With the height dependent precipitation distribution and the simplified temperature field it is possible to calculate the construction and reduction of snow coverage separately for each elevation band. Glacier covered areas are included separately, e.g. if there are snowless (aper) areas of the glacier snowmelt and icemelt are differentiated.

The required energy for meltwater production is not determined as a result of the energy balance because of the high amount of measurement and input meteorological sizes, like radiation and reflection. HBV3-ETH9 model uses the day-degree factor, and the energy for snowmelt is calculated directly from the air temperature. This will produce successful results if most of the energy comes from radiation and sensible heat flux. Therefore, the HBV3-ETH9 model needs a minimum of measured data.

The snowmelt water is estimated with the product of the current day-degree factor and the temperature difference of a specified period. The day-degree factor of a single day is estimated with the sinusoidal interpolation between CMIN (21st of December) and CMAX (21st of June). This takes the position of the sun and its impact on snowmelt into account.

The following simplified formulas are applied to estimate snowmelt:

$$CMELT = CMF \cdot (TM - T_0) \text{ (IV.3)}$$

CMELT = Amount of snowmelt (mm)

CMF = day-degree factor of single day (mm/(°C · d))

TM = Measured and interpolated mean daily temperature (°C)

T₀ = Threshold value temperature (°C)

IV.3.4 Estimation of intensity of orientation dependent ablation of snow cover

To estimate a more realistic ablation of snow cover it is important to distinguish between the orientations of the catchment. HBV3-ETH9 uses REXP as a parameter to consider the exposition dependent speed of ablation of snow cover for slopes facing south CMELT is multiplied with REXP; for slopes facing north CMELT is divided by REXP. East and west slopes are not differentiated on REXP.

A deviation of REXP = 1 (without consideration of orientation) has an effect on the form of runoff.

Figure IV.2 shows the reaction of the runoff with $REXP = 2$. Basis situation is a snow cover storage with equal water equivalent of snow cover in each orientation (this represents a simulation of snow cover without consideration of orientation). Figure IV.3 shows the superposition meltwater contribution of each orientation ($REXP = 2$) at an idealised catchment with all three equal parts of classes of orientation (south, north, west-east-horizontal). The resulting form of runoff is compared with an orientation independent snowmelt ($REXP = 1$).

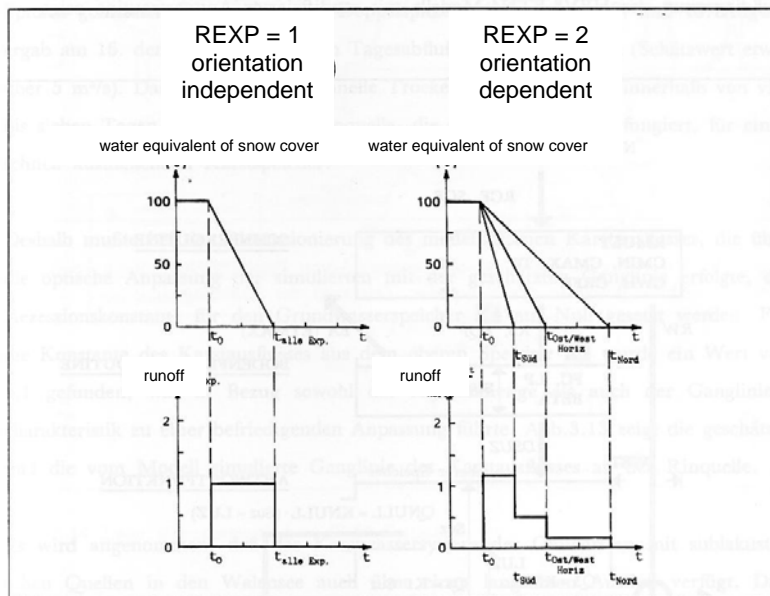


Fig. IV.2: schematic view of orientation dependent modelling of snowmelt and related form of runoff. (Hottelet 1991).

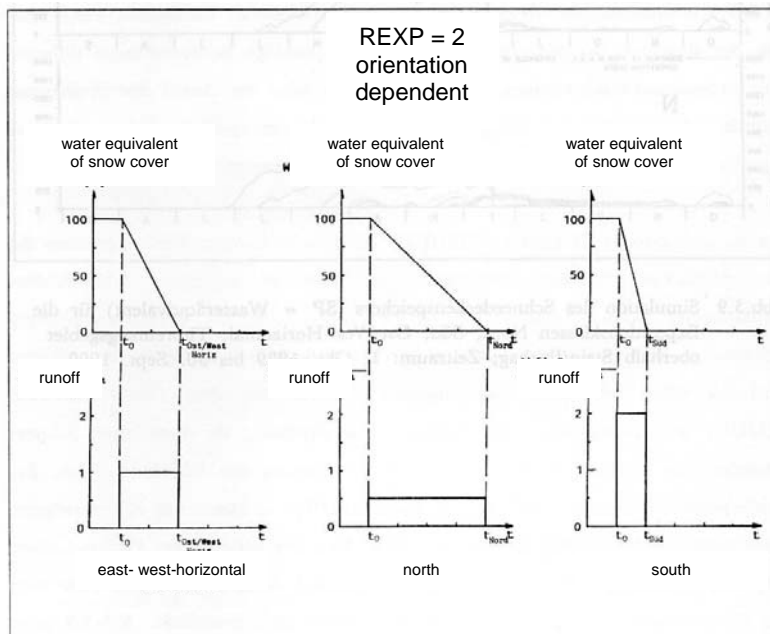


Fig. IV.3: comparison of resulting form of runoff of an orientation dependent ($REXP = 2$) and independent ($REXP = 1$) simulation of snowmelt in a schematic view; north : south : west-east-horizontal like 1 : 1 : 1. (Hottelet 1991).

IV.3.5 Estimation of storage and refreezing of liquid water in snow cover

Liquid precipitation or snowmelt results in liquid water in the snow cover. A portion of this water can be retained against gravity. CWH represents this storage of water in the snow cover.

$$SLIQMAX = CWH \cdot SP \text{ (IV.4)}$$

SLIQMAX	=	Maximum meltwater in snow cover (mm)
CWH	=	Retention
SP	=	Water equivalent of snowcover (mm)

If the sum of radiation balance and turbulent head flux is negative, liquid water can refreeze in the snowcover. CRFR determines the intensity of this process. The prerequisite for calculation of the "negative snowmelt" is: $TM \leq T0$.

$$CMELT = (TM - T0) \cdot CMF \cdot CRFR \text{ (IV.5)}$$

CMELT	=	Amount of snowmelt (mm)
CMF	=	day-degree factor of single day
TM	=	Measured and interpolated mean daily temperature (°C)
T0	=	Threshold value of temperature (°C)
IM	=	Steps per day; here = 1
CRFR	=	Refreezing coefficient

IV.4 Soil moisture routine and response function

The runoff model consists of the soil moisture routine and the response function.

The input into the soil moisture routine is the effective precipitation EQP. The two outputs are the influx into upper storage and the actual evaporation EA.

The Evaporation is calculated by the relative content of the soil moisture storage SSM and a seasonally variable amount of potential evaporation EP, found by optimisation. Prerequisite: $SSM \leq LP$.

$$EA = EP \cdot (SSM/LP) \text{ (IV.6)}$$

EA	=	Actual evaporation of a single day
EP	=	Potential evaporation of a single day
SSM	=	Soil moisture storage
LP	=	Upper limit of potential evaporation

The potential evaporation EP is estimated by a triangular function without evaporation from November till February. It starts on the 1st of March with a linear rise until the maximum is reached on the 30th of June and declines until 1st of November. The parameter to optimise is ETMAX.

The Output is the influx into the upper storage area, calculated as follows:

$$DSUZ = RS \cdot (SSM/FC)^{BETA} \quad (IV.7)$$

DSUZ	=	the influx into upper storage area (mm)
RS	=	Precipitation on landscape (mm)
SSM	=	Soil moisture storage (mm)
FC	=	Maximum soil moisture storage (mm)
BETA	=	Empirical coefficient controlling the outflow from soil moisture

The response function transfers the output of the soil moisture routine into runoff in one day steps. It consists of two storage areas, upper and lower, and a transformation function. The input is DSUZ and the precipitation on wetland RW. CPERC controls the flow from the upper to the lower storage area.

The output is Q0, Q1 and Q2. The transformation function calculates the runoff by these three parts.

The simulated runoff of the upper zone SUZ is the direct runoff. The direct runoff consists of overlandflow and interflow. DSUZ is the input into the upper storage area. SUZ expresses the unlimited filling level of the upper storage area. The outflow Q1 of the upper storage area is the interflow, controlled by K1, which expresses the daily amount of the storage level provided for outflow. If the storage level is higher than the threshold value LUZ the runoff Q0 is added, which is the overlandflow. The direct runoff is the sum of Q0 and Q1. For further details refer to figure IV.1.

The percolation is a further output of the upper storage area (prerequisite: CPERC > 0) into the lower storage area. The percolation is independent of the filling level of the upper storage area.

The lower storage area has two inputs, precipitation on wetlands RW and percolation from upper storage CPERC, as well as two outputs, potential evaporation EP and baseflow Q2. The precipitation on wetlands corresponds to the area of lakes and other wetlands WET, determined by cartography.

If the upper storage area is not dry the lower storage area gets constant, daily input by percolation. Q2 is the baseflow, which means the runoff of groundwater.

$$Q0 = K0 \cdot (SUZ - LUZ) \quad (IV.8)$$

$$Q1 = K1 \cdot SUZ \quad (IV.9)$$

$$Q2 = K2 \cdot SLZ \quad (IV.10)$$

Q0	=	overlandflow (mm/d)
Q1	=	interflow (mm/d)
Q2	=	baseflow (mm/d)
K0	=	storage discharge constants, upper zone
K1	=	storage discharge constants, upper zone
K2	=	storage discharge constants, lower zone
SUZ	=	upper zone storage (mm)

SLZ = lower zone storage (mm)
 LUZ = limit for fast drainage (mm)

Q2 represents the trend of the hydrograph, Q1 the amplitude of the hydrograph and Q0 creates the peaks of the calculated hydrograph (Renner 1991).

The transformation function generates the calculated runoff Q_{calc} by adding up the part runoffs Q0, Q1 and Q2 and distributing the runoff over several days. This distribution is realised by a triangular function defined by the of Q_{calc} . Due to the integration of the runoff height the concentration times and flow durations are considered (Bergström 1976).

IV.5 Calibration procedure

For calibration runoff values of adjacent hydrological years are used. The calibration period should reflect the whole climatic range of wet and dry years, as well as years of low and high snow coverage. Different criteria are useful to judge the fit of calculated and measured runoff. These criteria could be the accumulated difference between measured and calculated values, a visual inspection of plots with Q_{calc} and $Q_{measured}$ and a statistical criteria called Nash-Sutcliff coefficient, RSQ.

RSQ delivers a value up to 1. If RSQ is 1 the fit is perfect, which means that measured and calculated values are similar. If RSQ is less than zero the fit is poor. The Nash-Sutcliff coefficient can be estimated with the following equation.

$$RSQ = (F_0^2 - F^2) / F_0^2 \quad (IV.11)$$

RSQ = Quality value ($-\infty \leq RSQ \leq 1$); RSQ = 1 is the best fit
 F^2 = Sum of distance squares measured-calculated runoff
 F_0^2 = sum of distance squares of measured daily runoff and mean measured annual runoff.

F^2 and F_0^2 are calculated with the following equations.

$$F^2 = \sum (Q_m(t) - Q_c(t))^2 \quad (IV.13)$$

$$F_0^2 = \sum (Q_m(t) - mQ_m(t))^2 \quad (IV.14)$$

Q_m = measured runoff at instant t [m^3/s]
 Q_c = calculated runoff at instant t [m^3/s]
 mQ_m = mean measured runoff [m^3/s]

More information about RSQ can be found in Bergström 1976 and in Hottel 1991.

CHAPTER V RESULTS

V.1 General remarks

Once the meteorological input data are completed and the gabs are bridged the HBV3-Eth9 runoff model could be calibrated to the Langtang, Khumbu and Annapurna and Kanjiroba catchments.

The results presented in this chapter are temporarily and the calibration of the model parameters has to be improved to get better results.

V.2 Results of the different catchments

The presented results are a selection of calculated hydrological years of each catchment. The figures below show the comparison of measured and calculated discharge. The RSQ-value gives the quality of results as described in chapter VI. The corresponding calibrated parameters are given in a table at the end of each sub-chapter.

V.2.1 Langtang Khola, Langtang

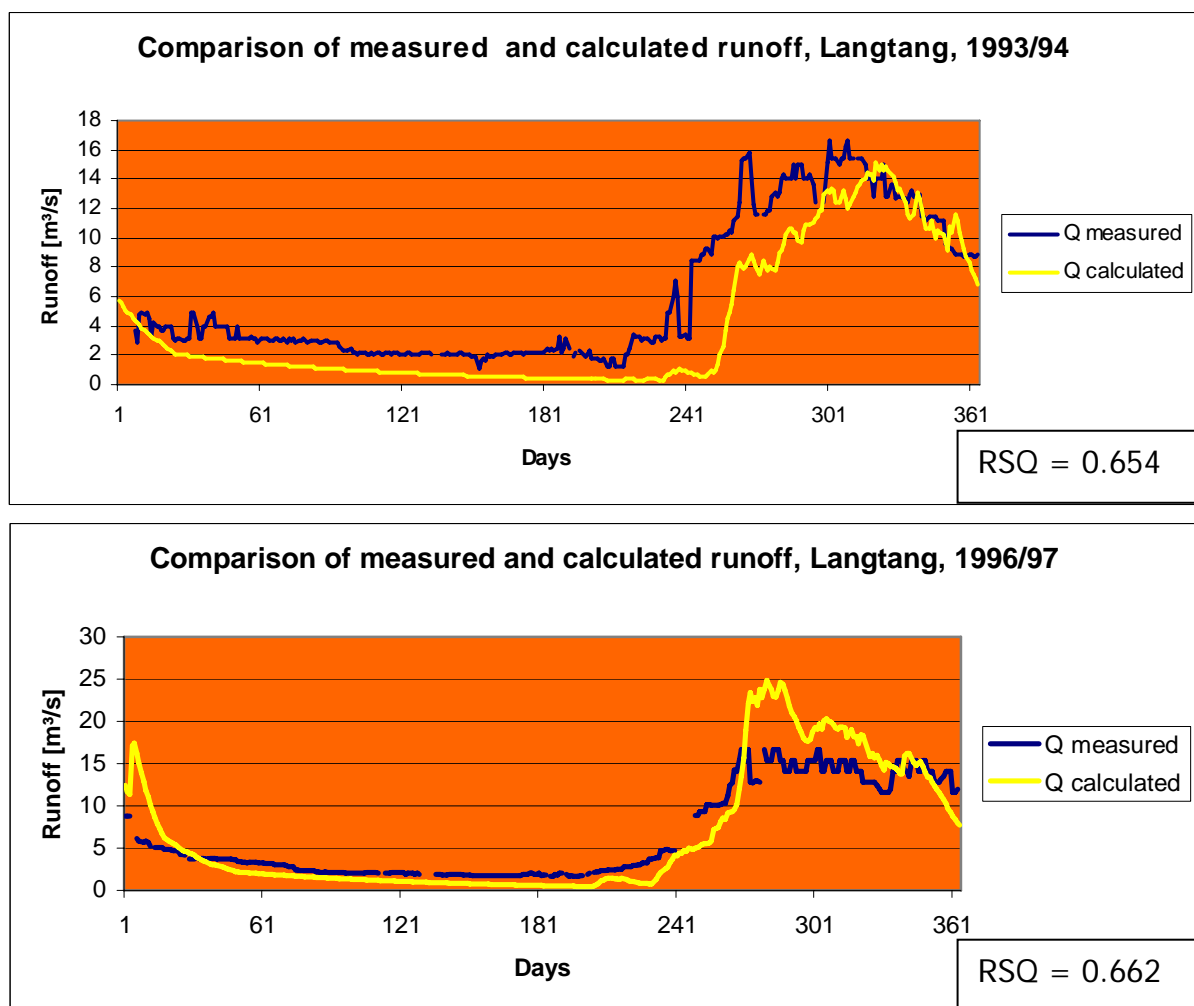


Fig. V.1: Results of runoff calculation of Langtang catchment, 1993/94 and 1996/97.

Tab. V.1: Calibrated parameters of Langtang catchment.

Parameter	Description of parameter	Value
BETA	Empirical coefficient controlling the outflow from soil moisture	0.16
CMAX	Maximum of degree-day factor	3.8
CMIN	Minimum of degree-day factor	2.3
CPERC	Percolation capacity into lower zone	0.6
CRFR	Refreezing coefficient	0.5
CROUTE	Parameter of transformation function	
CWH	Retention, coefficient of water holding capacity	0.82
ETMAX	Maximum of evapotranspiration	
FC	Maximum soil moisture storage, field capacity	164
K0	Storage discharge constants, upper zone	0.04
K1	Storage discharge constants, upper zone	0.04
K2	Storage discharge constants, lower zone	0.01
LP	Upper limit of potential evapotranspiration	152
LUZ	Limit for fast drainage, upper zone	25
PGRAD	Precipitation gradient	0.0
RCF	Rain correction coefficient	1.5
REXP	Increasing of snow-, ice melt depending on orientation of the slope	1.4
RMULT	Increasing melt of ice against snow	1.4
SCF	Snow correction coefficient	2.2
T0	Threshold value for transition of rain/snow and calculation of snowmelt	-0.4
TGRAD	Temperature gradient	-0.6

V.2.2 Modi Khola, Annapurna

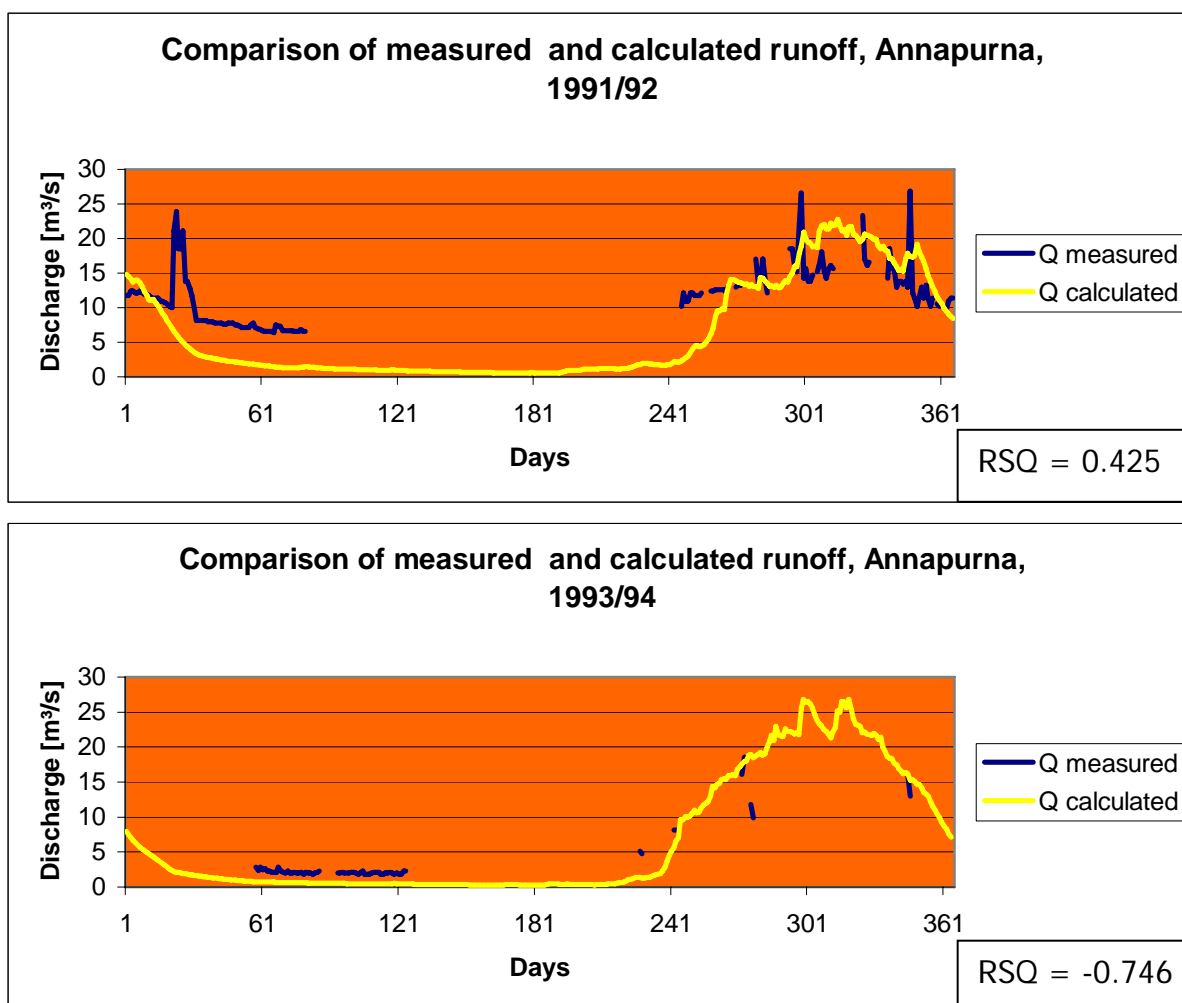


Fig. V.2: Results of runoff calculation of Annapurna catchment, 1991/92 and 1993/94.

Tab. V.2: Calibrated parameters of Annapurna catchment.

Parameter	Description of parameter	Value
BETA	Empirical coefficient controlling the outflow from soil moisture	0.17
CMAX	Maximum of degree-day factor	4.0
CMIN	Minimum of degree-day factor	5.0
CPERC	Percolation capacity into lower zone	0.45
CRFR	Refreezing coefficient	0.45
CROUTE	Parameter of transformation function	
CWH	Retention, coefficient of water holding capacity	0.1
ETMAX	Maximum of evapotranspiration	
FC	Maximum soil moisture storage, field capacity	165
K0	Storage discharge constants, upper zone	0.05
K1	Storage discharge constants, upper zone	0.03
K2	Storage discharge constants, lower zone	0.01
LP	Upper limit of potential evapotranspiration	183
LUZ	Limit for fast drainage, upper zone	27

PGRAD	Precipitation gradient	0.0
RCF	Rain correction coefficient	1.4
REXP	Increasing of snow-, ice melt depending on orientation of the slope	1.4
RMULT	Increasing melt of ice against snow	1.7
SCF	Snow correction coefficient	1.11
T0	Threshold value for transition of rain/snow and calculation of snowmelt	-0.6
TGRAD	Temperature gradient	-0.5

V.2.3 Imja Khola, Khumbu

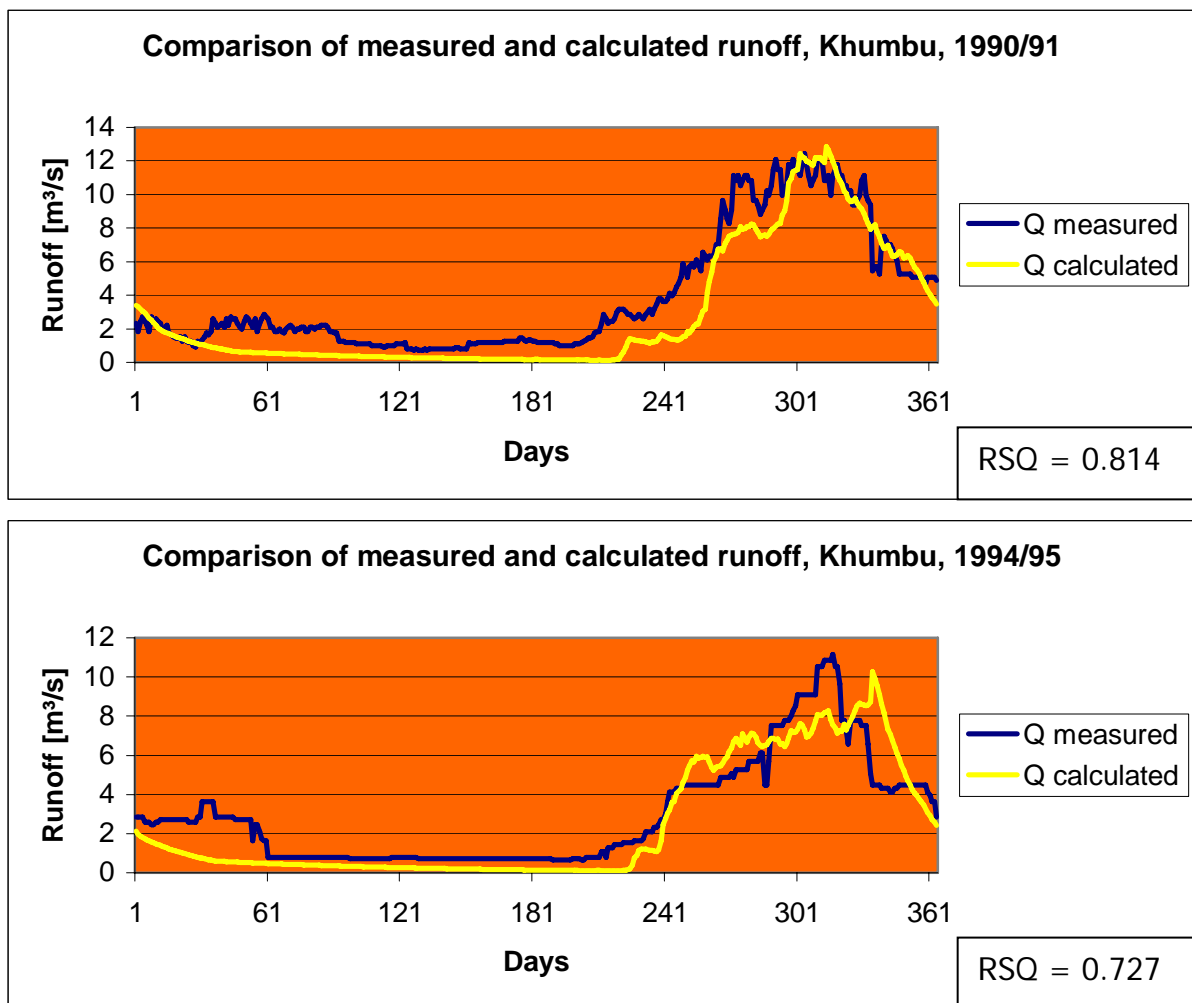


Fig. V.3: Results of runoff calculation of Khumbu catchment, 1990/91 and 1994/95.

Tab. V.3: Calibrated parameters of Khumbu catchment.

Parameter	Description of parameter	Value
BETA	Empirical coefficient controlling the outflow from soil moisture	0.17
CMAX	Maximum of degree-day factor	5.0
CMIN	Minimum of degree-day factor	4.0
CPERC	Percolation capacity into lower zone	0.45
CRFR	Refreezing coefficient	0.45

CROUTE	Parameter of transformation function	
CWH	Retention, coefficient of water holding capacity	0.1
ETMAX	Maximum of evapotranspiration	
FC	Maximum soil moisture storage, field capacity	165
K0	Storage discharge constants, upper zone	0.03
K1	Storage discharge constants, upper zone	0.03
K2	Storage discharge constants, lower zone	0.01
LP	Upper limit of potential evapotranspiration	183
LUZ	Limit for fast drainage, upper zone	27
PGRAD	Precipitation gradient	0.0
RCF	Rain correction coefficient	1.4
REXP	Increasing of snow-, ice melt depending on orientation of the slope	1.4
RMULT	Increasing melt of ice against snow	1.7
SCF	Snow correction coefficient	1.11
T0	Threshold value for transition of rain/snow and calculation of snowmelt	-0.6
TGRAD	Temperature gradient	-0.5

V.2.4 Sano Bheri, Kanjiroba

So far no simulation

ACKNOWLEDGEMENTS

The author is very thankful to Dr. L. Braun and his colleagues of the Commission of Glaciology at the Bavarian Academy of Science who encouraged me and initiated this project and gave scientific advice. Thanks go to the staff of the Snow and Glacier Hydrology Unit at the Department of Hydrology and Meteorology who provided all the required data. The author is indebted to Mrs. M. Shresta and Mr. B. Bajracharya of ICIMOD who gave valuable support with GIS and topographic information. This contact was made by Prof. Dr. S. Demuth.

The project was financed by the Federal Institute of Hydrology and by the Bavarian Academy of Science.

LITERATURE

Alford, D. (1992): Hydrological Aspects of the Himalayan Region. Kathmandu, Nepal: ICIMOD.

Bergström, S. (1976): Development and application of a conceptual runoff model for Scandinavian catchments. Bulletin Series A, 52.

Bergström, S. (1992): The HBV-model - its structure and applications
SMHI Hydrology Report No. 4, Swedish Meteorological and Hydrological Institute
Narrköping, Sweden.

Braun, L.N. and Renner, C.B. (1992): Application of a conceptual runoff model in different physiographic regions of Switzerland.
Hydrological Sciences-Journal 37, 3, p217-231.

Braun, L.N.; Grabs, W. and Rana, B. (1993): Application of a conceptual precipitation runoff model in the Langtang Khola basin, Nepal Himalaya. IAHS Publ. 218, 221-237.

Braun, L.N.; Hottelet, C.; Weber, M.; Grabs, W. (1998): Measurement and simulation of runoff from Nepalese head watersheds. IAHS Publ. 248, 9-18.

DAV (1990): Alpenvereinskarte, Langtang Himal, Ost. 1:50,000. Freytag – Berndt und Artaria Wien.

Escher-Vetter, H.; Weber M. und Braun, L.N. (1998): Gletscherverhalten als klimatische Information - Auswirkungen von Klimaänderungen auf den wasserhaushalt alpiner, teilweise vergletschertes Gebiete
BayFORKLIM Abschlußbericht, Met. Institut der LMU-München, auch als CD-Rom bei der KfG der BadW-München, sowie unter WWW.BADW.DE.

Grabs, W. and Pokhrel, A.P. (1993): Establishment of a measuring service for snow and glacier hydrology in Nepal – conceptual and operational aspects. IAHS Publ. 218, 3-16.

His Majesty's Government, Ministry of Land Reform and Management, Survey Department: National Geographic Information Infrastructure Programme (NGIIP). Digital Maps, Sheets. 2885-11, 2885-15, 2885-16, 2883-08, 2786-04, 2982-11, 2982-12, 2982-15, 2982-16.

Hottelet, Ch.; Braun, L.N.; Leibundgut, Ch. und Rieg, A. (1993): Simulation of Snowpack and Discharge in an Alpine Karst Basin
IHS Publication No. 218, p249-260.

ICIMOD and UNEP (2002): Inventory of glaciers, glacier lakes and glacier lake outburst floods monitoring and early warning systems in the Hindu Kush – Himalayan region. ISBN 92 9115 359 1.

Jauk, G. (2003): Gletscherschwund im Himalaya. Spektrum der Wissenschaft. August 2003. ISSN 0170-2971. Spektrum der Wissenschaft, Verlagsgesellschaft mbH, Heidelberg.

Kraus, H. (1988): The Climate of Nepal, Studies on the Climatology and Phytogeology of the Himalaya: Selections from Khumbu Himal. Kathmandu: Nepal Research Centre.

Renner, C.B. and Braun, L.N. (1990): Die Anwendung des Niederschlag-Abfluß Modells HBV3-ETH (V 3.0) auf verschiedene Einzugsgebiete in der Schweiz. Berichte und Skripten, Geographisches Institut ETH Zürich, 40.

Seibert, Jan (2002): HBV light version 2 User's Manual. Uppsala University Department of Earth Sciences Hydrology. E-mail: jan.seibert@ma.slu.se.

Shrestha, H.M. (1965): Our Rivers—A Preliminary Study in Gokhaptra (Magh 23, 2022).

Shrestha, H.M. (1985): 'Water Power Potential'. In Majupuria, T.C. (ed.) Nepal—Nature's Paradise, pp 32–38. Bangkok: White Lotus.

Shrestha, H.M. (1995): Hydropower in WECS, Supporting Document No. 2, Energy Perspective Plan.

Shankar, K. and Shrestha P.B.: (1985) 'Climate'. In Majupuria, T.C. (ed.) Nepal—Nature's Paradise, pp 39–44. Bangkok: White Lotus.

Spreafico, M. and Grabs, W. (1993): Determination of discharge with fluorescence tracers in Nepal Himalayas. IAHS Publ. 218, 17-27.

Schulz, M. (1999): Bestimmung der Wasserhaushaltsgrößen ausgewählter Einzugsgebiete mittels Messung und Simulation. Dipl. Arbeit, Institut für Geographie der LMU-München.

Weber, M. (1997): Aspekte zur Extrapolation von Tagesmittelwerten von Temperatur und täglichen Niederschlagssummen an hochgelegenen Gebirgsstationen aus Klimadaten des örtlichen Klimamessnetzes in Nepal. (Aspects of interpolating daily mean air temperature and daily precipitation sums for high elevation mountain stations based on climate data from the Nepalese Meteorological Service Network). Interner Bericht, Kommission für Glaziologie, Bayerischen Akademie der Wissenschaften, Munich.